Completion Report on the Production of Evapotranspiration Maps for Year 2006, Landsat Path 45 Covering the Upper Klamath and Sprague area of Oregon using Landsat Images and the METRIC^{tm} Model

Report by
Evapotranspiration, Plus
3496 N. 2500 E.
Twin Falls, ID 83301

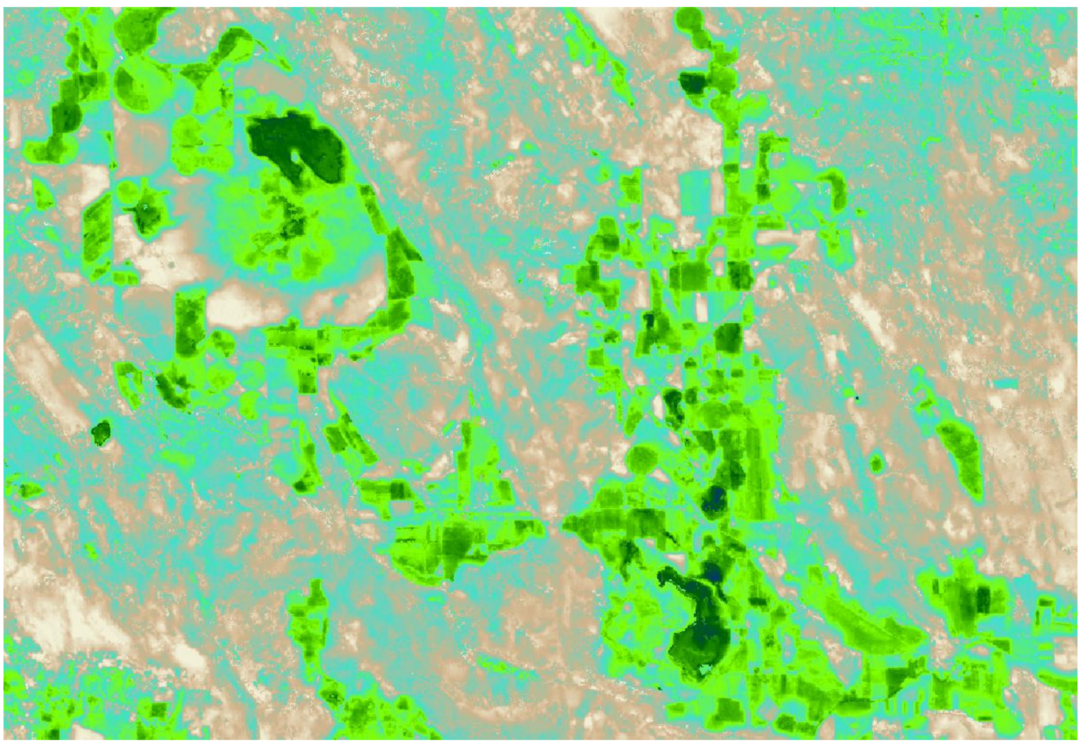

Growing Season ET for Irrigated Areas along the Upper Sprague River, 2006

Submitted to

US Geological Survey
Oregon Water Science Center
Portland, OR

May 2011

1. Introduction

This report describes the procedures for and products from processing satellite, weather and land-use data for the Landsat World Reference System (WRS) Path 45 covering portions of south-central Oregon containing agricultural and mountain areas from near Crescent, Oregon south to the Oregon-California border and containing land areas in the upper Klamath and the Sprague River basins. The purpose of the application was the production of spatial and temporal maps of monthly and growing season evapotranspiration (ET) for the region for the years 2004 and 2006. In this second report, products for 2006 are reported. The first report, submitted in March 2011, described similar production for year 2004.

The final products include 30 m resolution images of Actual Evapotranspiration (ET) and also images showing ET expressed as a fraction of Reference Crop ET (ET_rF). ET was calculated at the same 30 m spatial resolution as the Landsat satellite images. Nine Landsat images were processed along Landsat WRS path 45 by combining portions of WRS rows 30 and 31 to produce estimates of monthly and growing season (April – October) ET.

ET was obtained using the METRIC model developed by the University of Idaho. The METRIC procedure utilizes the visible, near-infrared and thermal infrared energy spectrum bands from Landsat satellite images and weather data to calculate ET on a pixel by pixel basis. Energy is partitioned into net incoming radiation (both solar and thermal), ground heat flux, sensible heat flux to the air and latent heat flux. The latent heat flux is calculated as the residual of the energy balance and represents the energy consumed by ET. The topography of the region was incorporated into METRIC via a digital elevation model (DEM), and used to account for impacts of slope and aspect on solar radiation absorption. METRIC was calibrated for each image using ground based meteorological information and identified 'anchor' conditions (the cold and hot pixels of METRIC) present in each image. A detailed description of METRIC can be found in Allen et al. (2007a,b; 2010).

Work by the University of Idaho (UI) during this project included further development of the METRIC model to perform more accurately under the specific conditions of the study area. Specific enhancements included a new cloud gap filling procedure for ET_rF[1] images that allows the operator to adjust for background evaporation occurring from recent precipitation to better reflect total evaporation over longer (monthly) periods, the generation of gridded ET_r maps used to estimate monthly and seasonal ET, improved computation of surface reflectance, albedo, terrain roughness and windspeed in mountainous areas to improve estimation of ET on sloped terrain. A description of the aerodynamic functions used in mountainous terrain is given in Appendix D. For Landsat 5 images, sharpening of the thermal band provided spatial refinement to the final ET products.

[1] ET_rF is the fraction of alfalfa reference ET_r as calculated by the standardized ASCE-EWRI Penman-Monteith equation (ASCE-EWRI, 2005) and represents the relative amount of reference ET occurring on any particular pixel of an image. ET_rF is a direct product from METRIC. ET_r is also used to calibrate the METRIC process and is calculated using hourly meteorological information from a weather station. Typical ranges for ET_rF are 0 to about 1.1. ET_rF is synonymous with the crop coefficient.

Figure 1a shows the domain of the Landsat images processed by METRIC for years 2006 and 2006. The image is a 'false composite' of bands 2, 3 and 4, where 'green vegetation' shows as a red color. Forest vegetation in mountainous areas show as dark red and broadleaf vegetation, including agricultural crops generally shows as a lighter red color.

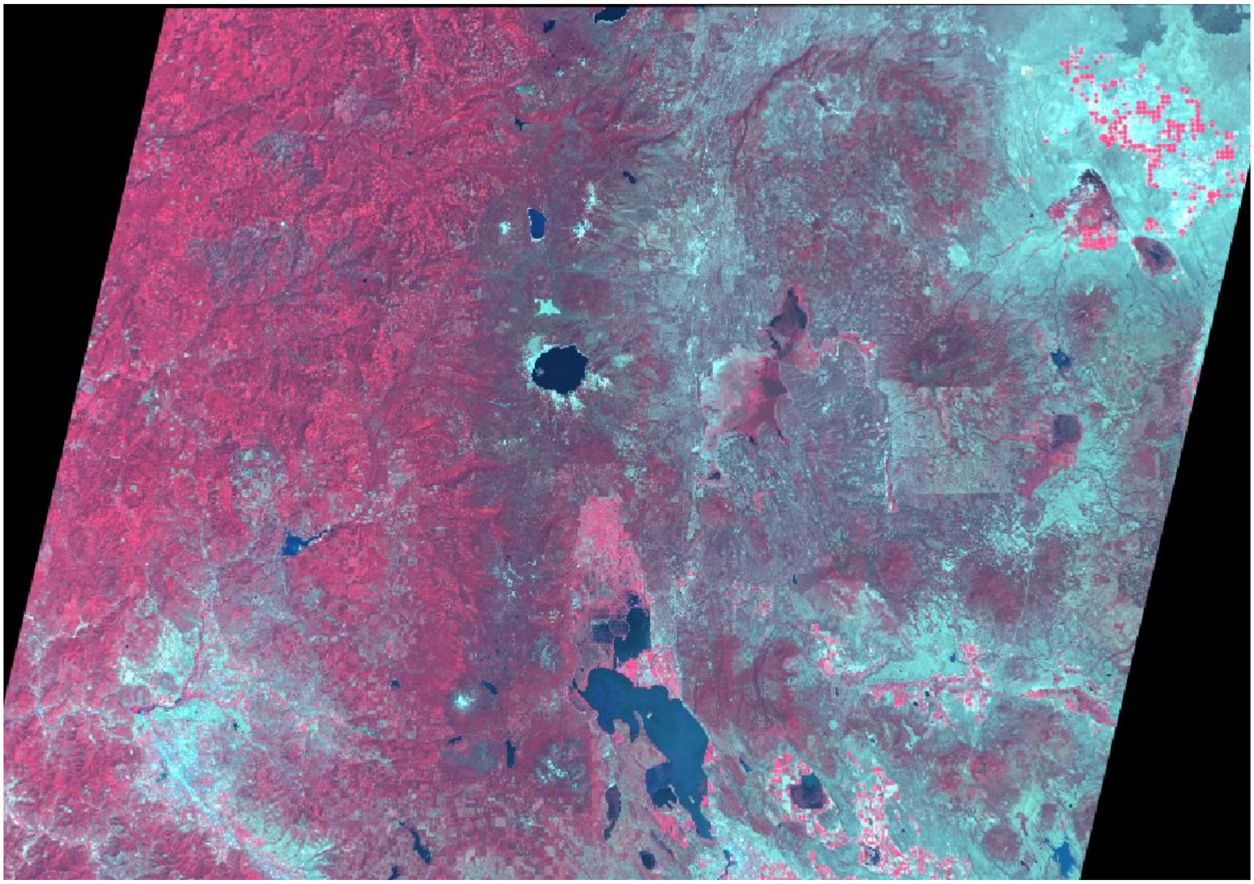

Figure 1a. False color composite Landsat image of path 45, rows 30 and 31 corresponding to 07/25/2006 showing the study area processed by METRIC.

Figure 1b shows an overlay on Landsat path 45, row 30 (southern portion) for the water basins of Williamson, Wood River/Upper Klamath Lake and Sprague, which are of interest to the USGS studies. The portion of row 31 of path 45 lying south of row 30, to the California state line, was added to the total area processed. That additional area, shown in Figure 1a, covers nearly all of the river basin domains shown in Figure 1b. The exception is a portion of the upper Sprague system that lies in path 44, east of path 45. That portion was estimated separately from METRIC using more simple vegetation index-based ET relationships that were derived from sampling of METRIC products from path 45. Landsat imagery was used in all cases.

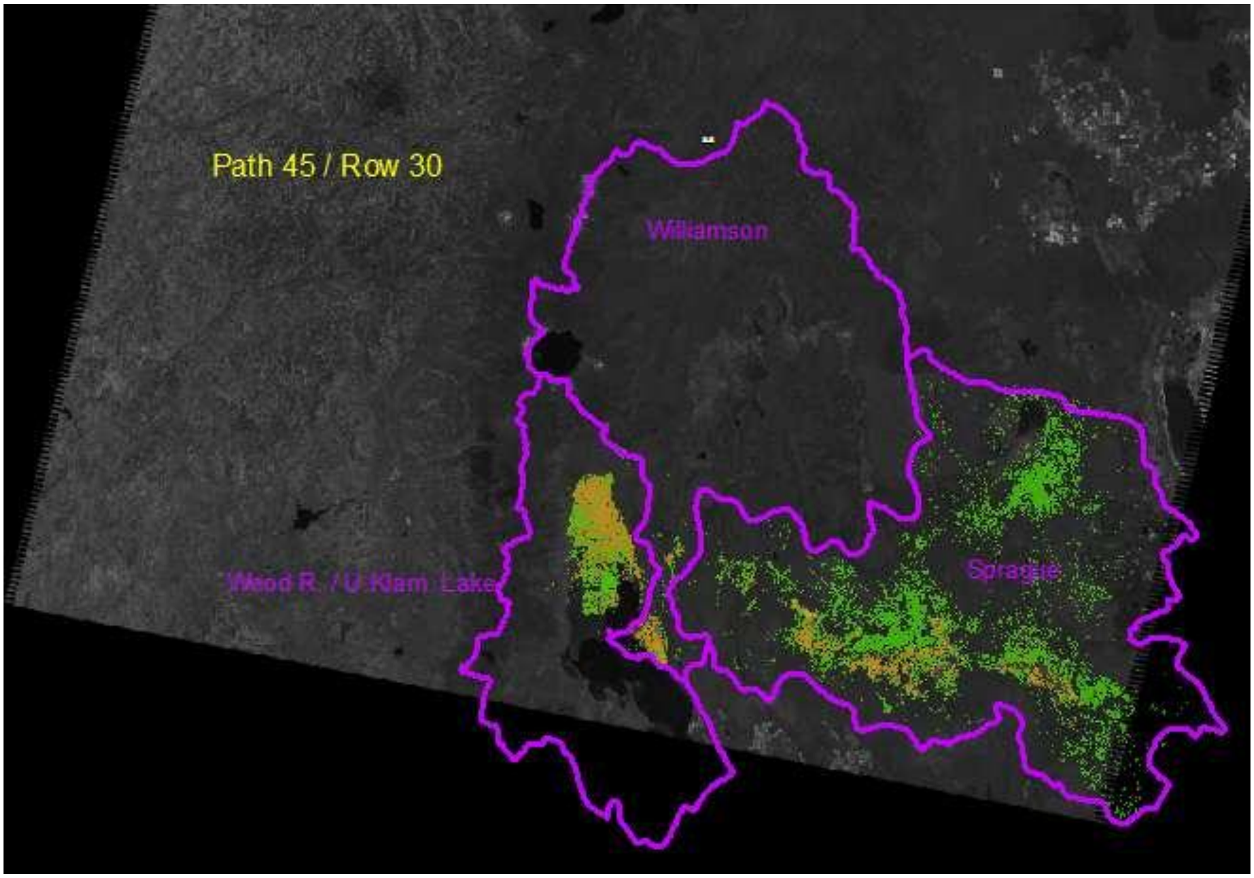

Figure 1b. Overlay of area of interest (purple lines) for ET processing and southern half of Landsat path 45, row 30 (courtesy of Daniel Snyder, USGS).

2. Image Selection and pre-processing

For this application, images from Landsat 5 and Landsat 7 satellites were utilized due to their high resolution and presence of a thermal band. The image archive for Landsat 5 dates back to 1984 and the satellite is still in operation. Landsat 7 was launched in 1999.

Landsat 7 images acquired after May 2003, although from a newer satellite than Landsat 5, are less preferred than Landsat 5, due to an anomaly with the Landsat 7 satellite caused by the malfunction of the scan line corrector (SLC). As a result, Landsat 7 images processed for years 2004 and 2006 are “SLC-off” images containing wedge shaped gaps extending from the edges of the image and stretching towards the centers. To obtain as complete coverage as possible, the gaps in ET_rF maps produced by METRIC are generally filled in during post processing using the natural neighbor tool of Arc-GIS. The Landsat 7 images were only used during periods when Landsat 5 images were not available due to clouds.

The most important criteria for the image selection is an assessment of cloud conditions at the time of the satellite overpass. The occurrence of conditions impeding the clearness of the atmosphere, such as clouds (including thin cirrus clouds and jet contrails), smoke, haze and similar over the study area may render parts of an image unusable for processing in METRIC. Even very thin cirrus clouds have a much lower surface temperature than the ground surface and because METRIC needs surface temperature estimates to solve the energy balance, areas with cloud cover cannot be used in the surface energy balance estimations. In addition, in cases of partial cloud cover, land areas recently shaded by clouds may be cooler as they have not yet reached a thermal equilibrium corresponding to the clear sky energy loading, and will also have to be masked out.

A total of 9 Landsat image dates were selected for METRIC processing for year 2006. These dates are shown in Table 1.

Table 1 – Dates of the Landsat satellite images used for METRIC processing in 2006.

#	Date	Image Type
1	04/28/2006	Landsat 7 ETM+
2	05/06/2006	Landsat 5 TM*
3	05/30/2006	Landsat 7 ETM+
4	06/23/2006	Landsat 5 TM
5	07/09/2006	Landsat 5 TM
6	07/25/2006	Landsat 5 TM
7	08/26/2006	Landsat 5 TM
8	09/27/2006	Landsat 5 TM
9	10/29/2006	Landsat 5 TM

Dem and Land Use maps used for METRIC processing

To enable processing with METRIC, other basic input files are needed besides the satellite images. METRIC requires the use of DEM (Digital Elevation Model) and LU (Land Use) files as inputs. A digital elevation map (DEM) is used during METRIC processing to adjust surface temperatures for lapse effects caused by elevation variation. Maps of slope and aspect (aspect is the cardinal direction of an inclined surface) are also derived from the DEM at 30 m resolution and are used in estimating solar radiation on slopes. These images were created using the tools of the ERDAS Imagine processing system based on the DEM.

A land use (LU) map was used to support the estimation of aerodynamic roughness and soil heat flux during METRIC processing. The NLCD (National Land Cover Database) Land Use map was obtained from the USGS-seamless webpage (http://seamless.usgs.gov/). The 30 m DEM was downloaded from the same website.

3. The METRIC Model

METRIC™ (Mapping Evapotranspiration with high Resolution and Internalized Calibration) is an ERDAS coded model that bases the ET estimate on the evaluation of the energy balance at the earth's surface. METRIC™ processes instantaneous remotely-sensed digital and weather data and estimates the partitioning of energy into net incoming radiation, heat flux into the ground, sensible heat flux to the air, and latent heat flux. The latent heat flux, which is computed as a residual in the energy balance, represents the energy consumed by ET:

$$LE = Rn - G - H$$

where LE=latent energy consumed by ET; Rn=net radiation; G=sensible heat flux conducted into the ground; and H=sensible heat flux convected to the air. One very strong advantage of using energy balance is that actual ET rather than potential ET based on amount of vegetation is computed so that reductions in ET caused by a shortage of soil moisture are captured. A disadvantage of the energy balance approach is in the complexity of calculations. In traditional applications of energy balance, the computation of LE is only as accurate as the summed estimates for Rn, G, and H. METRIC attempts to overcome this disadvantage by focusing the internal calibration on LE and with H used to absorb all intermediate estimation errors and biases.

METRIC™ utilizes spectral raster images from the visible, near infrared, and thermal infrared energy spectrum to compute the energy balance on a pixel-by-pixel basis. In METRIC, Rn is computed from the satellite-measured narrow-band reflectance and surface temperature; G is estimated from Rn, surface temperature, sensible heat flux and vegetation indices; and H is estimated from surface temperature ranges, surface roughness, and wind speed using buoyancy corrections. Figure 2 shows a general schematic of the METRIC process.

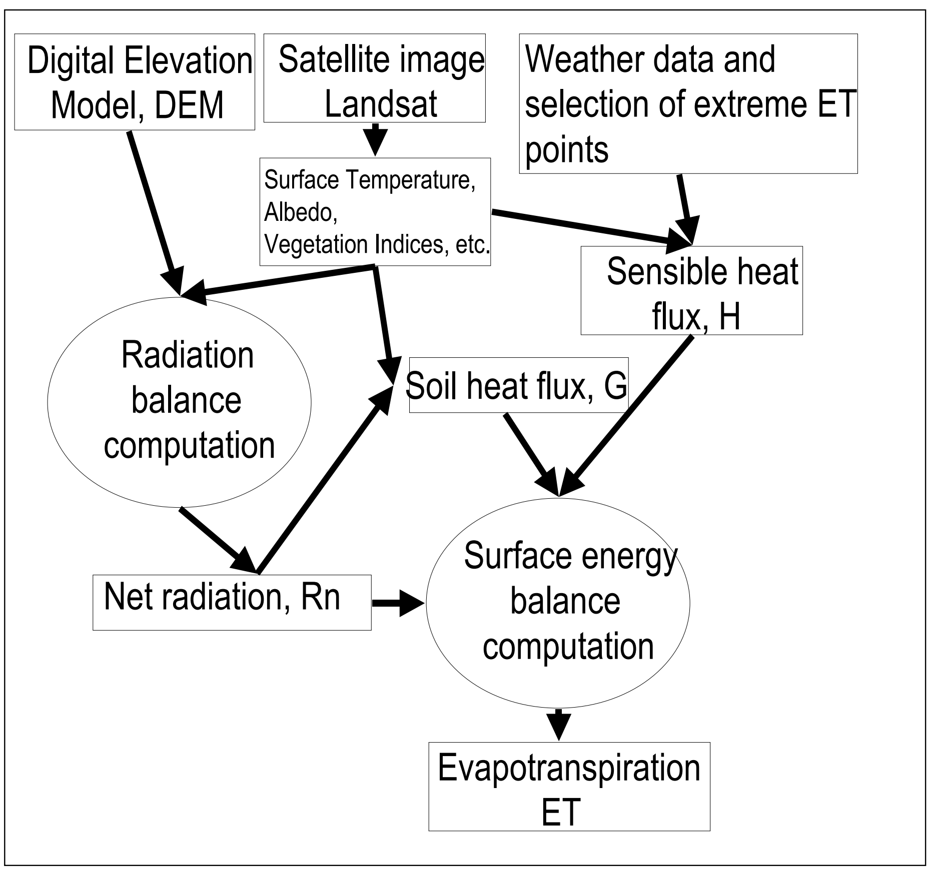

Figure 2. General schematics of the METRIC process.

Calibration of METRIC

METRIC version 2.0.5 was used for the UI processing, but with some modifications during 2010 and early 2011. The 2.0.5 version was released by the University of Idaho in January 2010. A detailed description of METRIC can be found in Allen et al. (2007a,b) and Allen (2008).

The main focus for the processing was to generate estimates of ET from lands having agricultural production, so that METRIC was calibrated with primary focus on accurate estimation of ET from the agricultural areas. However, because the full Landsat images were processed, efforts were made to minimize uncertainty in ET estimates from other land cover types present within the image, including forests, riparian vegetation and rangeland.

Calibration Philosophy.

METRIC uses a vertical near surface-to-air difference, dT, to estimate sensible heat flux. Sensible heat flux (H) is the amount of heat that is convected from a surface into the air, thereby reducing the amount of available energy for evaporation. The dT function is modeled as linearly proportional to surface temperature and is defined using the properties of two user selected anchor pixels, the "cold" and the "hot" pixels, that represent the extreme conditions encountered within the image (a condition having nearly complete conversion of available energy into evapotranspiration and a condition having nearly zero conversion of available energy into evapotranspiration). The cold anchor pixel generally represents a fully vegetated and actively transpiring vegetation, while the hot anchor pixel represents a bare and dry or nearly dry agricultural soil with little or no vegetation. The selection of cold and hot anchor pixels by the user is described by Allen et al., (2007b) and Allen (2008). These pixels are generally selected from agricultural fields for consistency and to match assumptions made in the estimation of soil heat flux, for example, where that algorithm was developed for agricultural soils. The surface temperature used to estimate dT was 'delapsed' to account for differences in surface temperature occurring as a result of elevation differences.

During the internal calibration of sensible heat flux in METRIC, a fraction of ET_r, ET_rF, is assigned to the hot and cold conditions. ET_rF is equivalent to the crop coefficient (K_c) based on full-cover alfalfa as the reference crop. ET_rF at the cold pixel is normally assigned a value of 1.05 (Allen et al., 2007a,b) unless vegetation cover is insufficient to support this assumption (for example, early in spring and during winter when full, robust vegetation cover is rare). The 1.05 assignment to ET_rF is used to account for the variation in ET inherent within a large population of fully vegetated fields. Previous applications of METRIC and comparisons against lysimeter measurements of ET at Kimberly, Idaho show that the "nearly coldest", or wettest, agricultural fields having full vegetation cover tend have ET rates that are typically 5% higher than that of the alfalfa reference ET_r. This is because, for a large population of fields, some fields may have a wet soil surface beneath the canopy, or the canopy may be wet from recent (sprinkler) irrigation or precipitation, that tend to increase the total ET rate to about 5% above ET_r. In addition, when viewing a large population of fields containing full cover alfalfa, a specific subpopulation of fields will have somewhat wetter conditions and therefore slightly higher ET and slightly cooler temperature than the "mean" full cover condition represented by the alfalfa reference. When the METRIC image is calibrated using an ET_rF of 1.05 at the cold pixel, sampling of ET_rF over a large population of full cover, irrigated fields tends to produce, on average, an ET_rF value of 1. The cold pixel is selected from a population of fields having full cover and relatively cold temperatures. Ideally, an alfalfa field is preferred for calibration, since the ASCE Penman-Monteith equation is calibrated to an alfalfa reference. However, Wright (1982) has shown that most agricultural crops, when at full cover, transpire at levels very similar to those of alfalfa. Therefore, the selected location for the cold pixel does not need to be alfalfa, but can be any pixel from within the interior of a fully vegetated, cool, field (crop type is generally unknown when applying METRIC).

During calibration of METRIC via the assignment of ET_rF values for the cold and hot pixel conditions, normally only a single weather station is utilized in the calibration. A single station is used during calibration for several reasons. One, the locations for the cold and hot conditions are selected as close as possible to the single calibration weather station (usually within 20 km) so that wind speed and reference ET from the station can be assumed to closely approximate that for the selected calibration pixels. The internal calibration of the sensible heat flux function within METRIC is tied to the wind speed occurring at the calibration locations. Secondly, the internal calibration of the sensible heat flux function within METRIC generally requires the use of the same wind speed as was used in its determination, throughout the image. Third, the assignment of the ET_rF at the hot pixel is closely tied to any recent precipitation occurring at the calibration weather station. Fourth, the assignment of ET_rF at the cold and hot pixel conditions and the application of the METRIC process to the image should create (if calibrated and applied correctly) an ET_rF surface over the image that has general limits of 0 and 1, and that can be later applied to an ET_r surface that may vary over the image.

Special Calibration Cases.

Table 2 summarizes locations, NDVI and ET_rF values assigned for cold and hot pixel conditions. For 4/28/2006, 5/06/2006 and 5/30/2006, the daily surface soil water balance run using data from the Agency Lake weather station indicated residual evaporation from recent rain events. The water balance suggested values of ET_rF = 0.22, 0.20 and 0.22, respectively, for the bare soil condition for the three dates. These values were used to represent the driest bare soil conditions in the image area surrounding the calibration weather station (Agency Lake) to adjust the calibration for the presence of the background evaporation. The other image dates were estimated from the daily soil water balance to have reached a relatively dry state, where only residual, diffusive evaporation, estimated at ET_rF = 0.10, was occurring. The daily soil water balance is shown later in Figure 6.

Table 2. ET_rF values assigned to and locations (X, Y coordinates in UTM meters zone 10 WGS1984) for the hot and cold pixels for each image date.

Date		**X**	**Y**	**NDVI**	**ETrF**
4/28/2006	cold	594420	4720470	0.705	0.95
	hot	589710	4702770	0.124	0.22
5/06/2006	cold	592260	4719300	0.787	1.05
	hot	589620	4702740	0.148	0.2
5/30/2006	cold	589740	4707060	0.763	1.05
	hot	587070	4702980	0.150	0.22
6/23/2006	cold	585180	4701930	0.786	1.05

	hot	590250	4679400	0.126	0.1
7/09/2006	cold	590010	4705650	0.800	1.05
	hot	599010	4677600	0.149	0.1
7/25/2006	cold	587610	4706700	0.837	1.05
	hot	589920	4711560	0.200	0.1
8/26/2006	cold	587640	4706790	0.836	1.05
	hot	587760	4703640	0.139	0.1
9/27/2006	cold	597210	4690110	0.807	1.05
	hot	588510	4703370	0.180	0.1
10/29/2006	cold	587190	4707360	0.774	1.05
	hot	586830	4705860	0.143	0.1

4. Weather data processing

METRIC utilizes alfalfa reference ET (i.e., ET_r) as calculated by the American Society of Civil Engineers (ASCE) standardized Penman-Monteith equation (ASCE-EWRI 2005) for calibration of the energy balance process and to establish a daily soil water balance to estimate residual soil evaporation from bare soil following precipitation events (Allen et al., 2007a). The ET_r is used as a means to 'anchor' the surface energy balance by representing the ET from locations having high levels of vegetation and cooler surface temperatures. Therefore, high quality estimates of ET_r are needed, which, in turn, require high quality weather data. Therefore, before processing the satellite images, the quality and accuracy of the meteorological data were assessed.

Hourly weather data time steps are needed to produce ET_r for calibration of the METRIC energy balance estimation process at the time of the Landsat overpasses. The hourly ET_r values are summed to daily totals to provide a basis for producing daily and monthly ET. ET_r was calculated using the RefET software (version 3) of the University of Idaho (Allen, 2008).

Quality Assessment and Quality Control of the Weather Data

To apply METRIC, reference ET is calculated from weather data sets having the following parameters, plus some of these parameters are used in the METRIC calibration:

- Wind speed (hourly average): for computation of sensible heat flux (wind speed at satellite overpass time is required) and reference evapotranspiration (ETr) with the REFET software.
- Precipitation (24 hour): to evaluate evaporative soil moisture conditions at the satellite overpass time.
- Dew point temperature (hourly average): for calculation of atmospheric transmissivity and instantaneous incident solar radiation (clear sky) at satellite overpass time. Also used for reference ET calculation.
- Incident solar radiation (hourly average): for reference ET calculation
- Air temperature (hourly average): maximum and minimum temperature for reference ET calculation.

Before being used for these calculations, QA (Quality Assessment) and QC (Quality Control) procedures as recommended by ASCE-EWRI (2005) were applied to investigate the general quality of data. In the case of solar radiation, for example, measured values (hourly or daily) were compared to estimated clear sky solar radiation taken as the upper bound for measured. Sensor malfunctioning, calibration problems, low maintenance and other issues can lead measured values to have systematic bias. Such systematic errors can be corrected based on expected clear sky conditions. Adjustments are applied by means of appropriate coefficients. In Figure 4 good agreement between registered solar radiation (Rs) and theoretical clear-sky solar radiation (Rso) indicates appropriate calibration of the sensor at Agency Lake for the date shown.

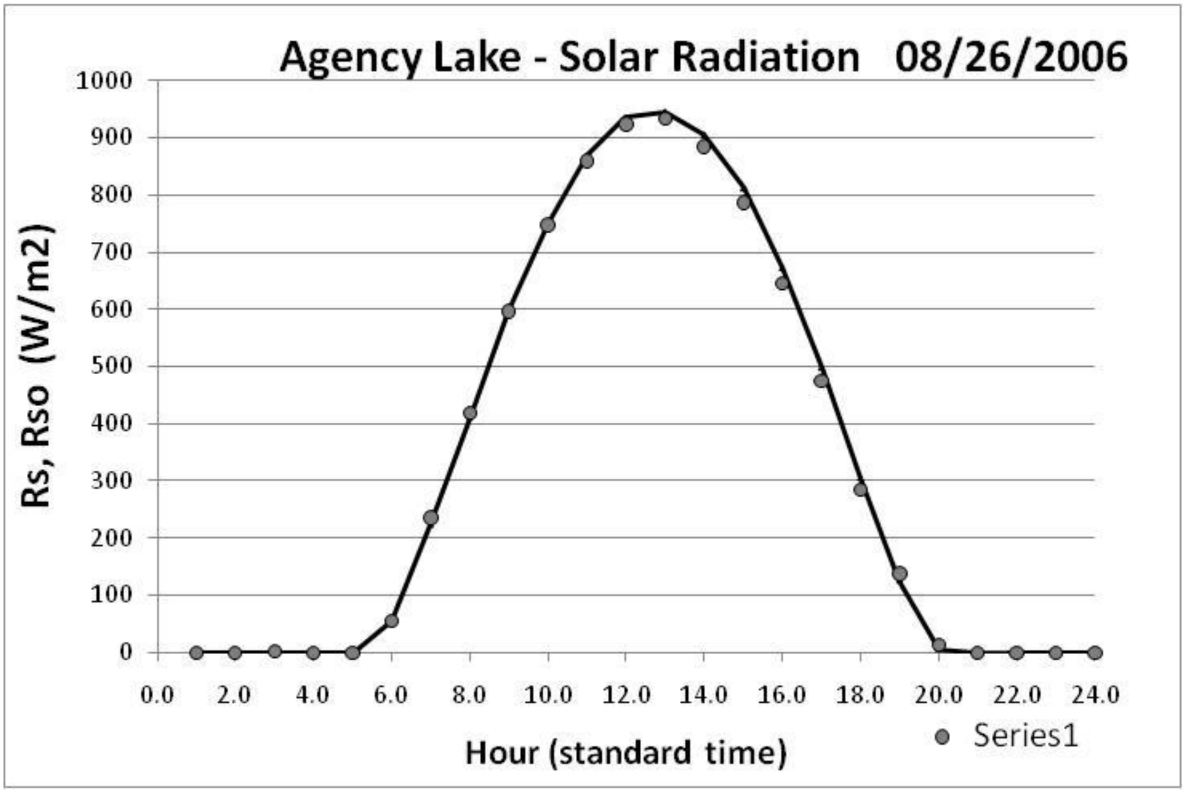

Figure 4. Solar radiation (Rs) plotted against theoretical clear-sky solar radiation (Rso).

In Figure 5 a plot of hourly mean air temperature and dewpoint is shown for a 24-hour period. In agricultural settings one can expect the recorded minimum temperature to be close to the dewpoint temperature observed at the same time, as in the case in the figure shown for 8/26/2006.

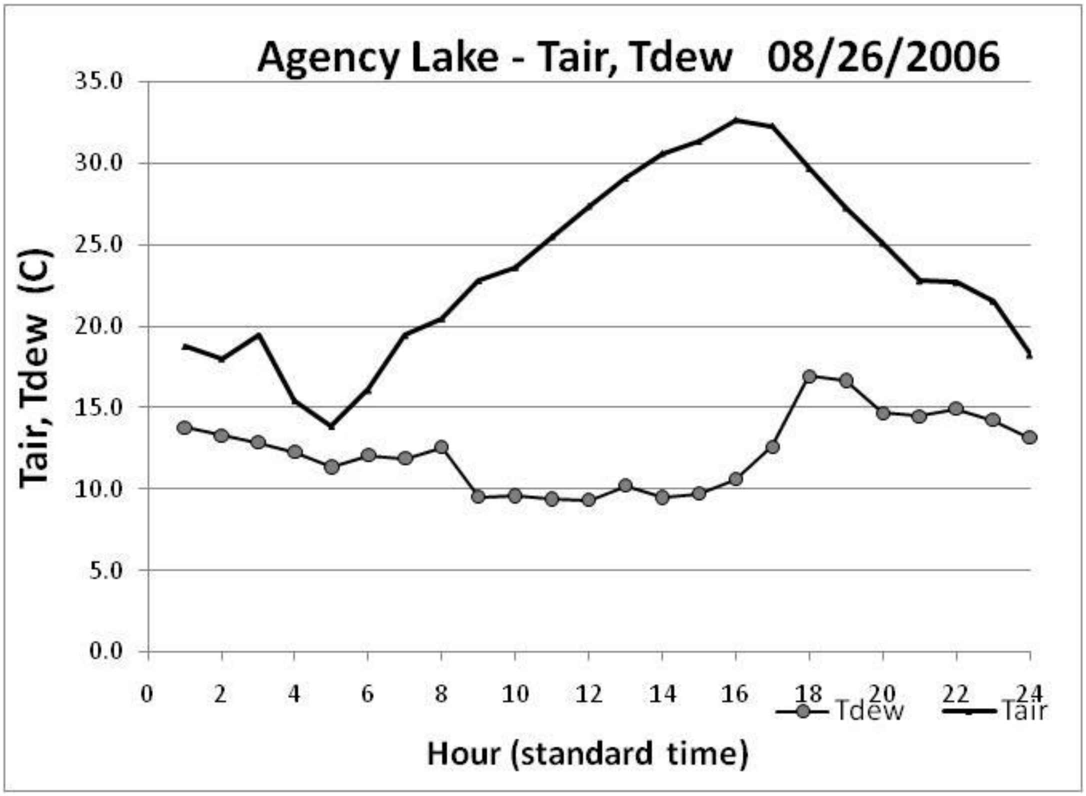

Figure 5. Air temperature and dew point temperature registered at AGENCY LAKE on 8/26/2006

5. Using a daily soil water balance model for METRIC calibration.

A daily soil water balance was applied to the 2006 period using precipitation and ET_r data from the Agency Lake weather station. The water balance estimates residual evaporation from a bare soil surface on each image date as shown in Figure 6. The soil water balance is based on the two-stage daily soil evaporation model of the United Nations Food and Agriculture Organization's Irrigation and Drainage Paper 56 (Allen et al., 1998). Fig. 6 shows a simulation of evaporation from the upper 0.125 m of soil at Agency Lake.

During the drying cycle after a wetting event, a typical bare agricultural soil can be expected to continue to evaporate at a small rate beyond the first several weeks due to diffusion of liquid water and vapor from beneath the upper soil layer. This evaporation can continue at very low rates for several additional weeks, provided no new wetting events occur, especially from tilled soils that have a moderate amount of water stored within the soil profile. This is typical of agriculture.

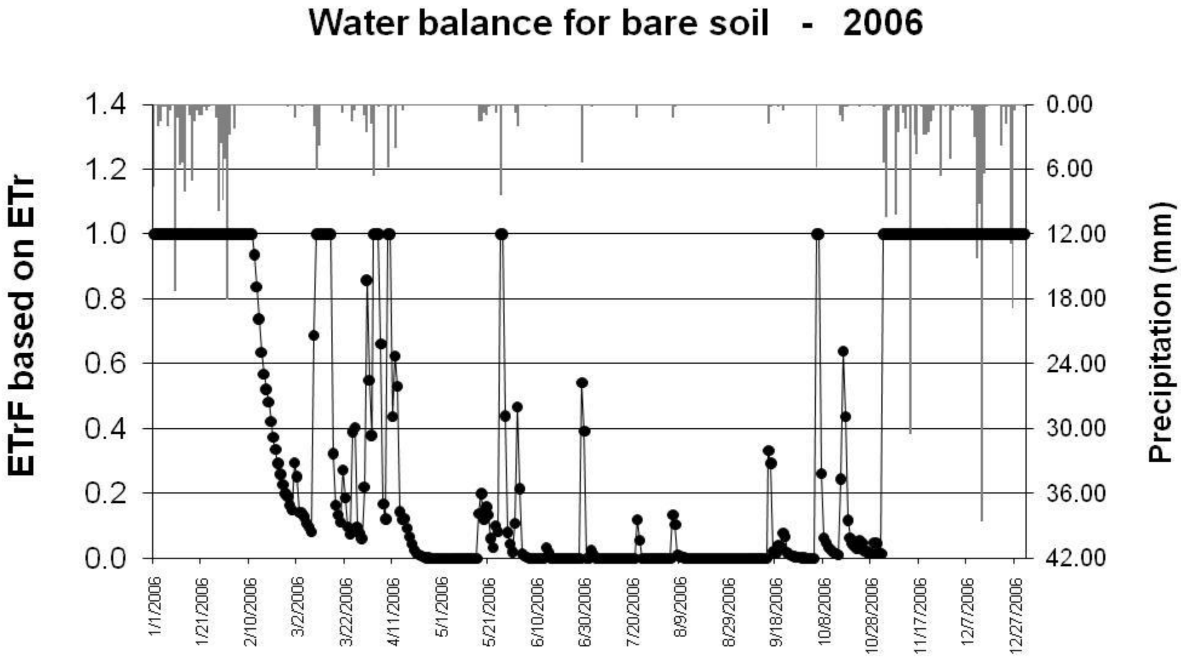

Figure 6. Daily ET_rF for bare soil estimated from the soil water balance for 2006 using weather data from the Agency Lake weather station.

6. METRIC™ processing and results

METRIC produces 30x30 m spatial resolution maps of both ET_rF (Fraction of Reference Evapotranspiration) and actual ET. The main products produced by METRIC are:

- Instantaneous ET_rF and ET maps, at satellite time for every image.
- Daily ET_rF and ET maps, for every image.
- Monthly ET_rF and ET maps .
- Seasonal ET_rF and ET maps.

Intermediate Products

During the METRIC™ process, dimensionless vegetation indices (NDVI, LAI and NDWI), surface reflectance (albedo), and surface and DEM-delapsed temperature maps are created. NDVI (normalized difference vegetation index) and LAI (leaf area index) maps are used in METRIC™ as indicators of biomass and aerodynamic roughness, and as predictors of ratios of soil heat flux to net radiation or sensible heat flux. The LAI is defined as the total one-sided green leaf surface area per unit ground surface area. The typical range for LAI is zero to six, where zero represents bare soil and greater than four represents dense vegetation. LAI values above three represent “full cover” conditions, and generally imply maximum ET in well irrigated areas.

NDVI is calculated as the relative difference in reflectance between the shortest near infrared band (band 4) and the red band (band 3), respectively:

$$\mathrm{NDVI} = \frac{\rho_4 - \rho_3}{\rho_4 + \rho_3}$$

where $\rho 3$ and $\rho 4$ are the at-satellite reflectances in bands 3 and 4 respectively. NDVI is somewhat sensitive to the color of the soil, spectral bandwidth, and atmospheric attenuation. Typically, NDVI varies between 0.1 and 0.8, with the higher value indicating dense vegetation and values less than about 0.2 associated with soil/rocks. Negative NDVI values typically indicate water bodies and snow, which reflect more energy in the red spectrum than in the near infrared.

NDWI (normalized difference water index) is calculated as the relative difference at satellite reflectance between bands 5 and 2

$$\mathrm{NDWI} = \frac{\rho_5 - \rho_2}{\rho_5 + \rho_2}$$

where $\rho 5$ and $\rho 2$ are the at-satellite reflectances in bands 5 and 2 respectively. This is an index defined for the identification of water bodies. A value lower than zero indicates the presence of water bodies. In combination with NDVI, NDWI produces a good map of watery areas.

Lapse rate

In METRIC, the simulation of DEM delapsed temperature is necessary for estimating the near surface temperature gradient (dT) used to estimate sensible heat flux. This requires the establishment of an atmospheric lapse rate. For the area of study a unique lapse rate was used on each image date for elevations less than 1750 m, to represent lapsing trends along the agricultural valleys inside the image; this lapse rate is called the “flat” lapse rate during METRIC processing. Another lapse rate was used for elevations greater than 1750 m that represents mountainous conditions; this one is called the “mountain” flat rate. Unique values were sometimes required for specific images, determined by operator observation of surface temperature trends. Common (standard) values for the lapse rates are 6.5 K/1000 m for the ‘flat’ rate and 10 K/1000 m for the ‘mountain’ rate where K is degrees Kelvin.

Refinements to the METRIC Mountain Model

The METRIC model gives special treatment to mountainous areas and areas of other steep terrain during the computation of solar radiation inputs, where the influences of slope and aspect on energy inputs are calculated, and during the computation of convective heat exchange (H), where influences of slope and terrain roughness on estimated wind speed and aerodynamic transport are estimated. During the application to the Klamath region, additional refinements were made to both reflectance estimation (that uses solar radiation estimates as inputs) and to aerodynamic components. These refinements improved the behavior of the algorithms for both north and south facing steep slopes along the Cascade Range. The refinements to aerodynamics are described in Appendix D. Refinements to reflectance calculations were to parse solar radiation, by band, into beam, diffuse and terrain reflectance components during estimation of slope and aspect effects, and then reassembling the components prior to calculating reflectances. The result was improved estimation of reflectances on steep, north-facing slopes.

Sharpening

Although the final products from METRIC are of high spatial quality when produced from Landsat imagery, an even finer resolution for the images is often desirable, especially when ET within individual field parcels is needed. Landsat 5 images have 120 m spatial resolution of longwave (thermal) band that is coarser than the 30 m for coincident shortwave bands, and the 120 m thermal information tends to dominate the resolution of the final ET product. To improve the quality of the results, a procedure known as *sharpening* was applied to the final individual ET_rF images generated with the METRIC code. This procedure is described in the METRIC manual (Allen et al., 2010) and in a paper by Trezza et al. (2008).

The basic sharpening philosophy and procedure followed is based on the application of an established Surface Temperature (Ts) vs NDVI relationship to produce a first estimate of Ts at every short wave pixel, assuming a linear relationship and correspondence between NDVI and Ts. Later, to preserve original Ts information, this first estimate of Ts is adjusted so that Ts averaged over all shortwave pixels lying within an original thermal pixel matches the original average Ts of that thermal pixel. In most of the cases the redistribution of the bias between the original thermal Ts and the estimate Ts is an iterative process.

Figure 7 shows an example of an ET_rF map for a Landsat scene from 2004, before and after sharpening surface temperature. This procedure was applied to all Landsat 5 images to enhance the resolution of the final ET_rF product. Landsat 7 images were not sharpened because they are already at 60 m resolution.

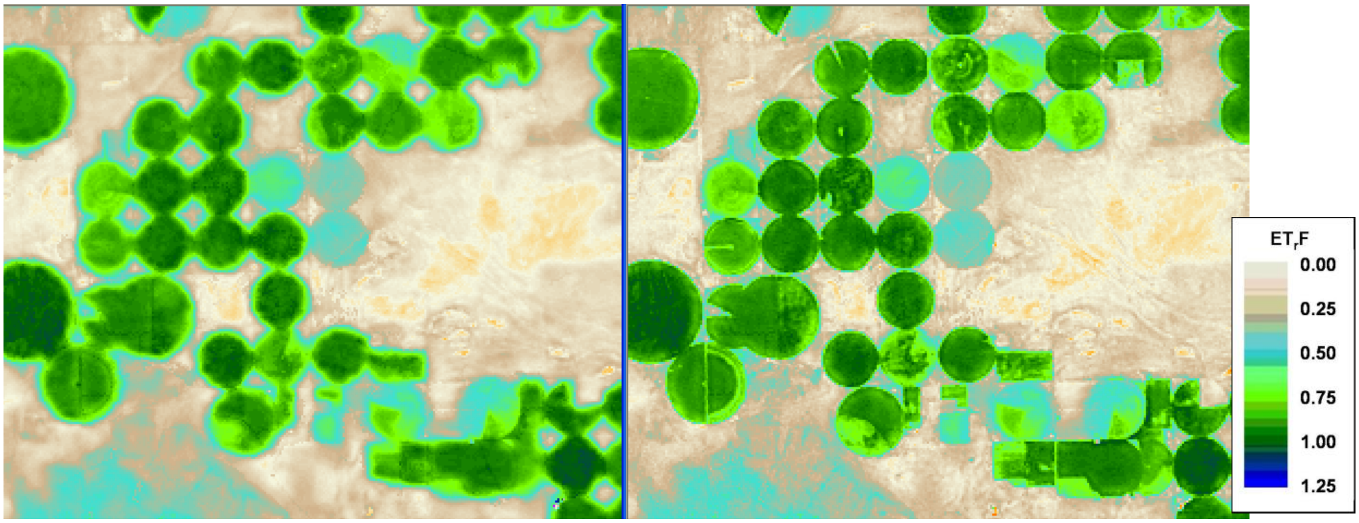

Figure 7. Left: Close-up of ET_rF image from path 45 corresponding to June 17th 2004; the area is close to Christmas Valley, OR. Right: The same ET_rF map but using sharpened surface temperature.

Gapfilling for Landsat 7 images

Landsat 7 images acquired after May 2003 have information gaps caused by the malfunction of the scan line corrector. As a result, Landsat 7 images processed for year 2004 and 2006 are "SLC-off" images where wedge shaped gaps exist in the images, extending from the edges of the image and stretching towards the centers. To obtain as complete coverage as possible, the gaps in ET_rF maps produced by METRIC were filled in during post processing using the natural neighbor tool of Arc-GIS. Figure 8 shows a close-up of an area along the Sprague River from 2004, where the natural neighbor interpolation procedure was applied. The quality of the interpolation depends on the location of the gap, being better over homogenous landscapes.

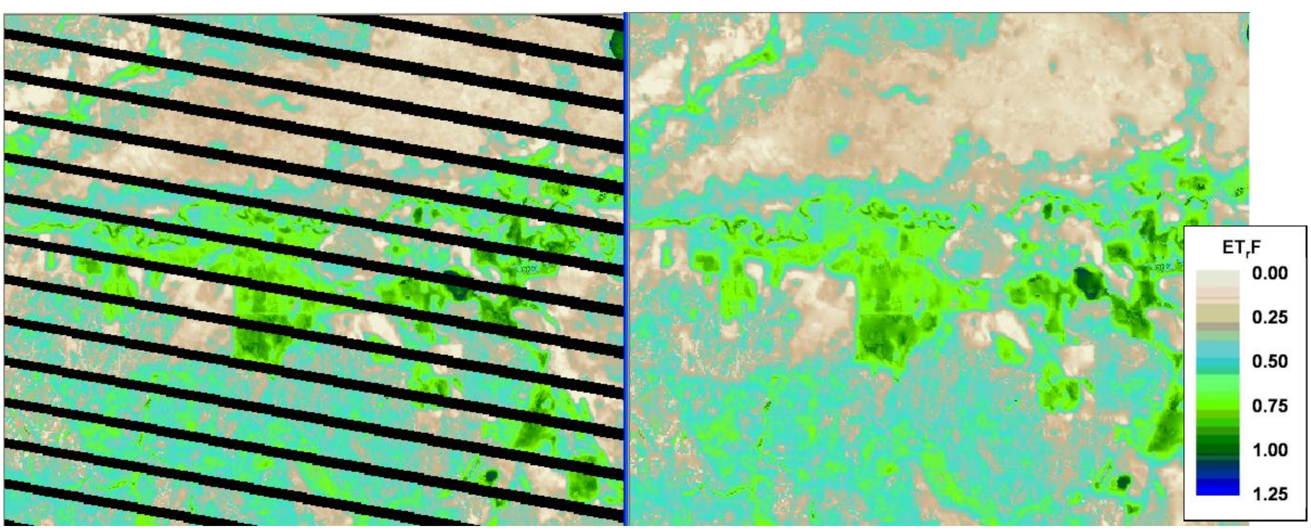

Figure 8. Left: Close-up of ET_rF image corresponding to July 11th 2004, showing gaps (stripes) originated from the Landsat 7 image; the area is close to Sprague River. Right: The same ET_rF map, after gaps were filled using natural neighbor interpolation.

Daily ET_rF products

METRIC was applied for every image included in Table 1 to obtain instantaneous (at satellite) and daily ET_rF maps. As previously described, a total of 9 images were processed (Table 1).

Maps of reflectance of short wave radiation, vegetation indices (NDVI and LAI), surface temperature, net radiation and soil heat flux were generated as intermediate products during METRIC processing. The final output from the METRIC energy balance model were images showing instantaneous ET_rF (fraction of alfalfa based reference ET, ET_r) at the satellite overpass time. For land covers other than rangeland, the estimate of daily ET_rF was set equal to the instantaneous at the satellite overpass time, based on extensive ET measurements made using precision weighing lysimeters at Kimberly, Idaho (Allen et al., 2007b; Allen, 2008).

The following section presents a view of each instantaneous ET_rF image, with some comments in the figure captions (figures 9 – 17).

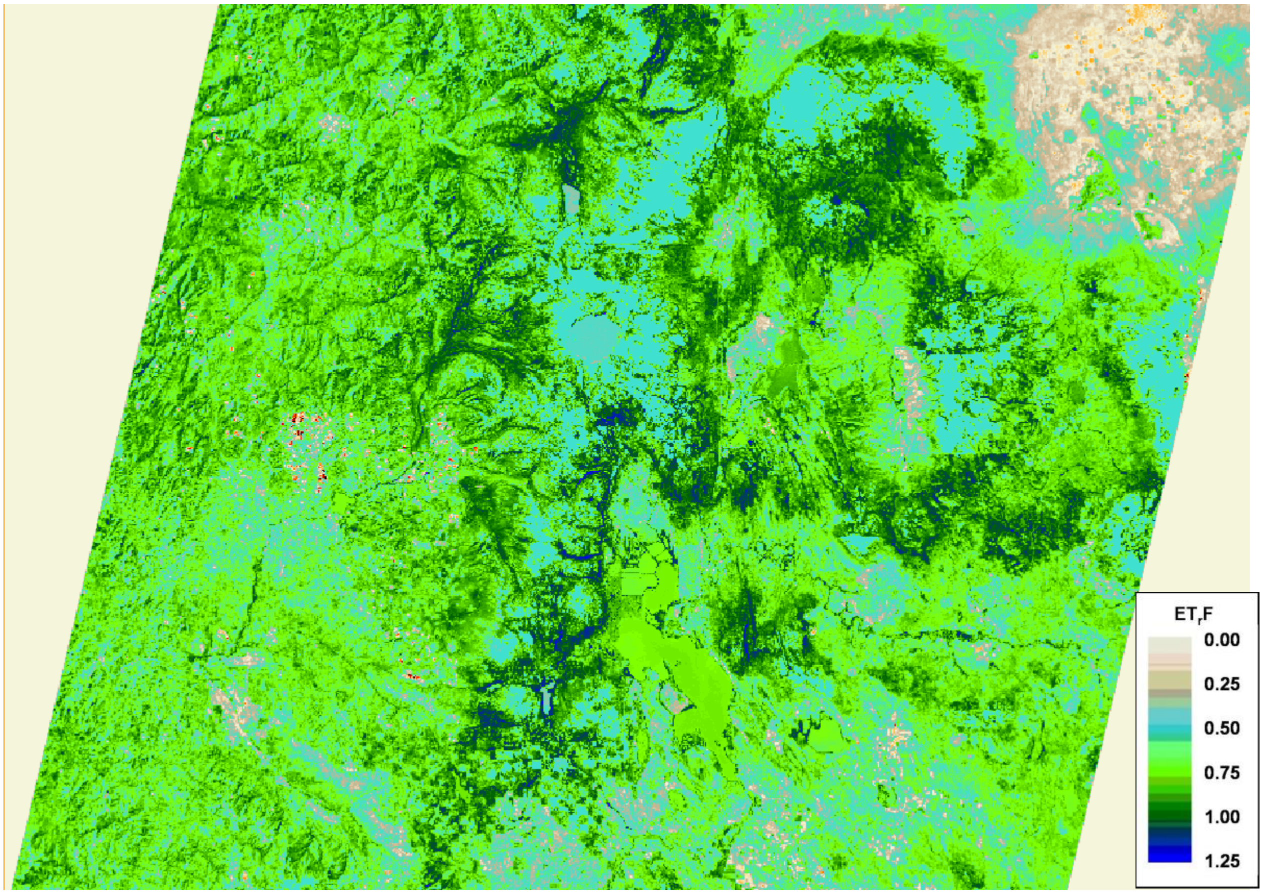

Figure 9. ET$_r$F map for 04/28/2006. Masked cloudy areas are identified as black. The image shows the product after filling the gaps in the Landsat 7 image. Snow-covered areas are shown as a turquoise, where an ET$_r$F value of 0.5 was used to approximate the sublimation from snow. Mountainous areas were relatively 'wet,' with lower-lying agricultural areas more dry.

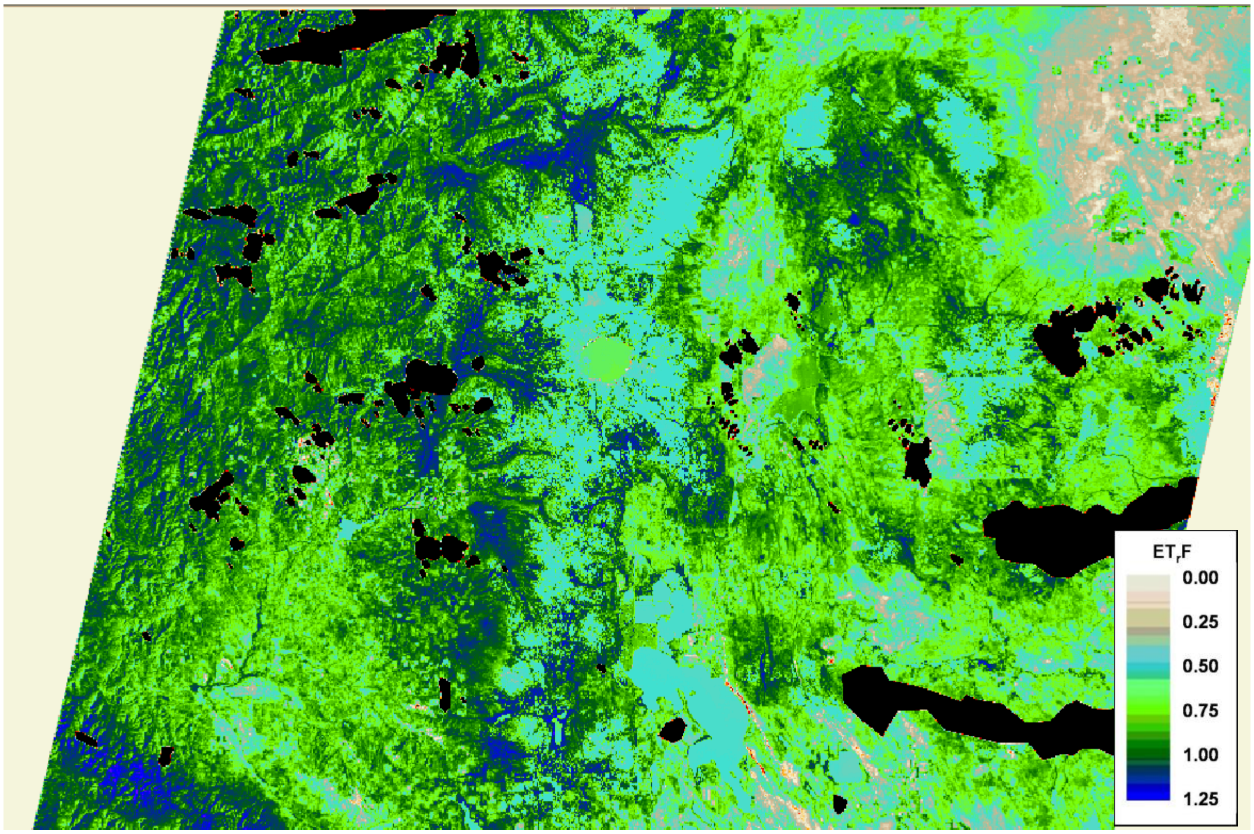

Figure 10. ET_rF map for 05/06/2006. Masked cloudy areas are identified as black. This image was relatively wet in the mountainous regions, with drier conditions in agricultural areas.

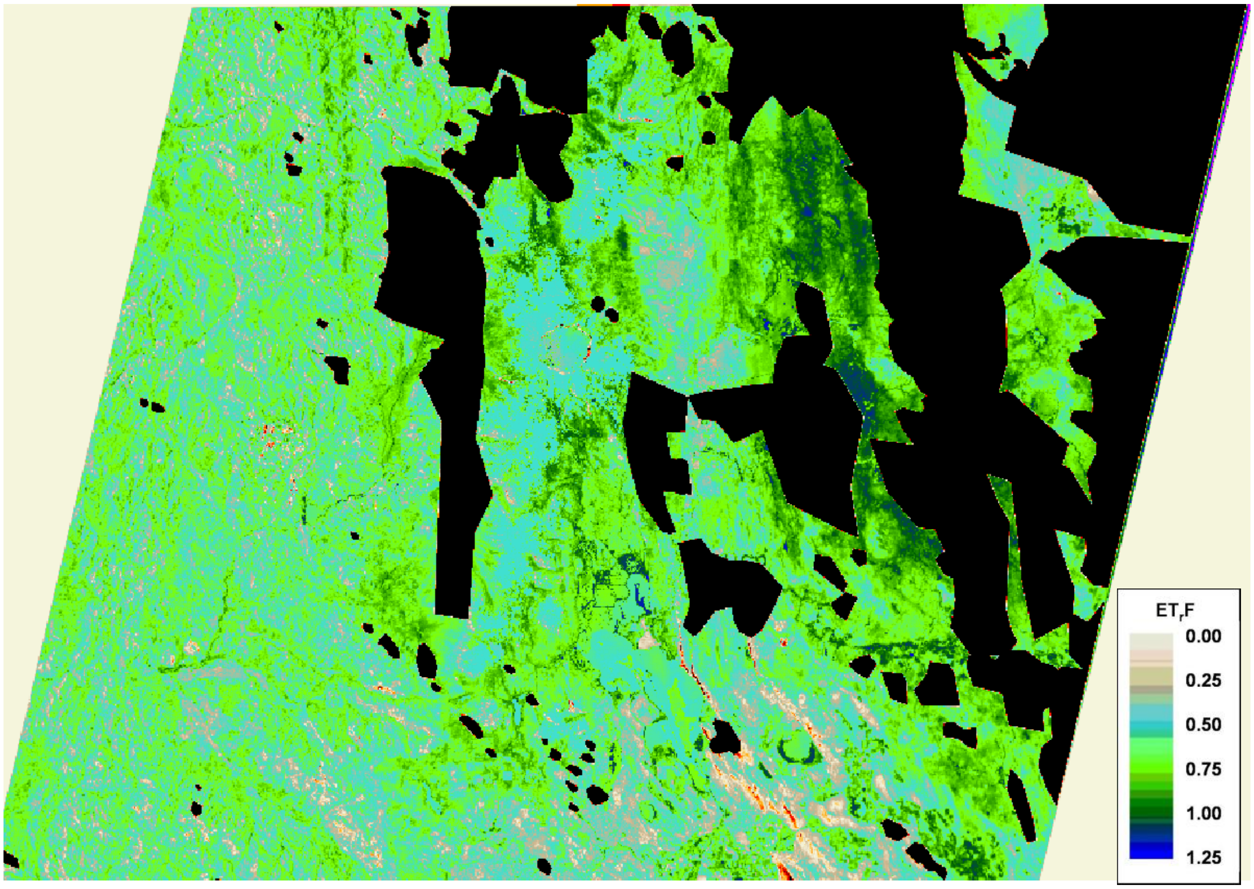

Figure 11. ET$_r$F map for 05/30/2006. Masked cloudy areas are identified as black. The image shows the product after filling the gaps from the Landsat 7 image.

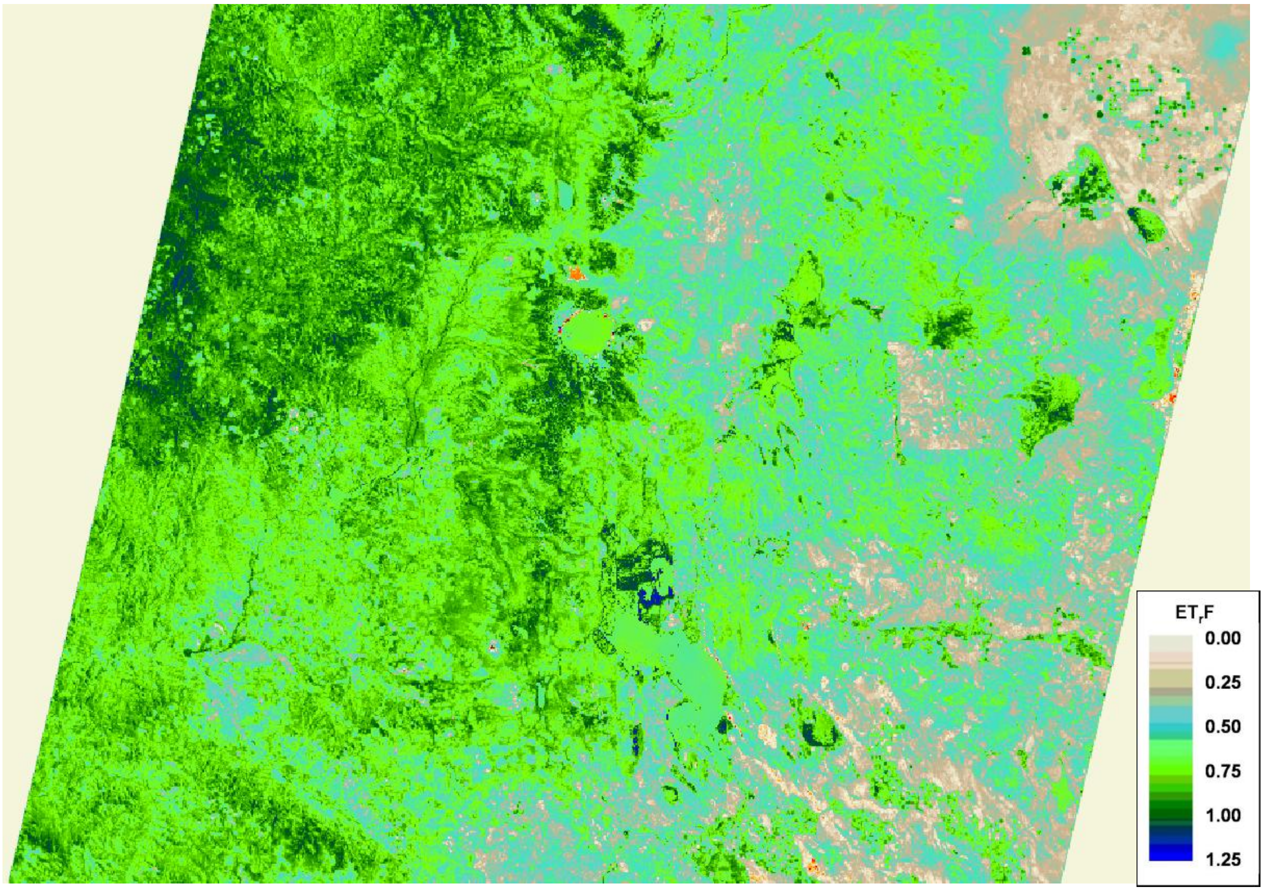

Figure 12. ET$_r$F map for 06/23/2006. Masked cloudy areas are identified as black. Lower lying areas that are not irrigated have dried considerably. Transpiration is shown to remain strong in mountainous regions.

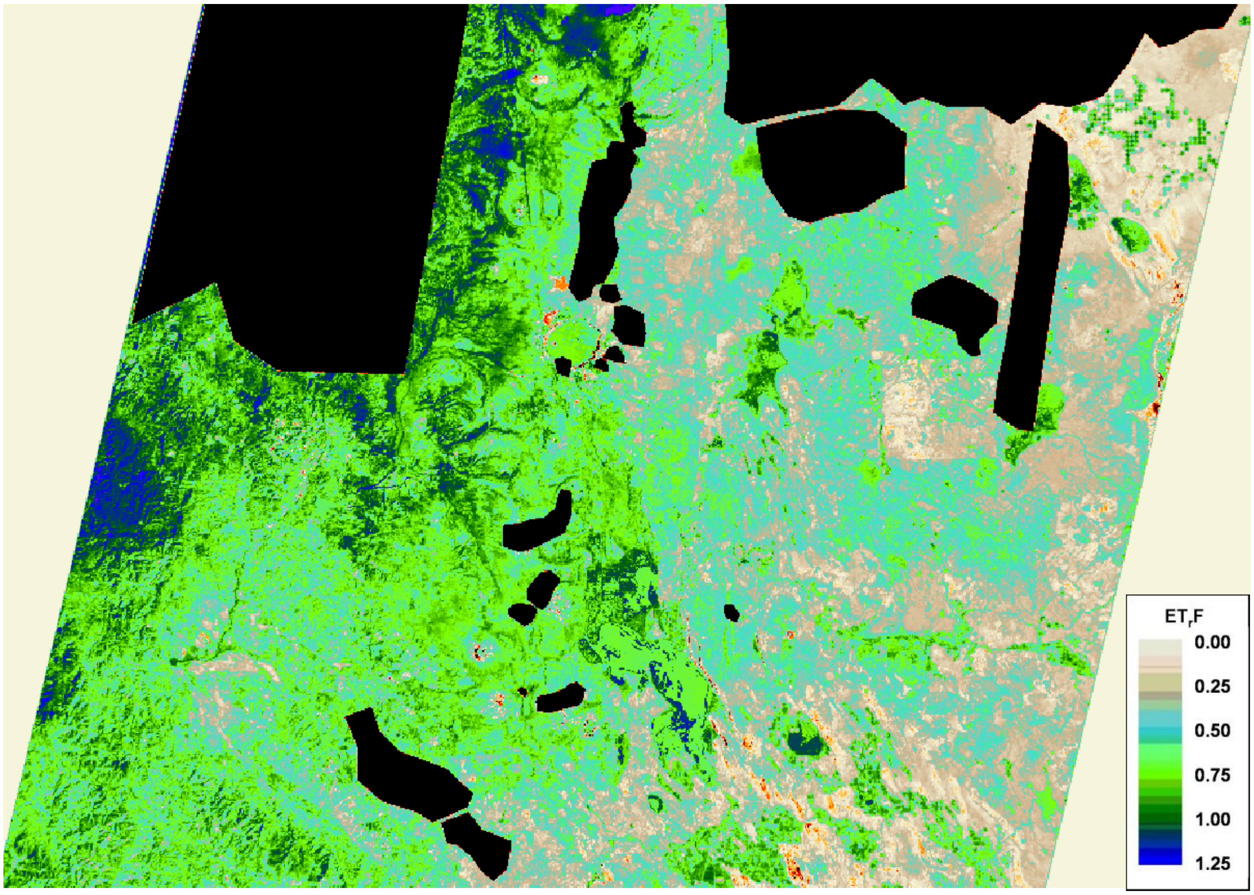

Figure 13. ET_rF map for 07/09/2006. Masked cloudy areas are identified as black.

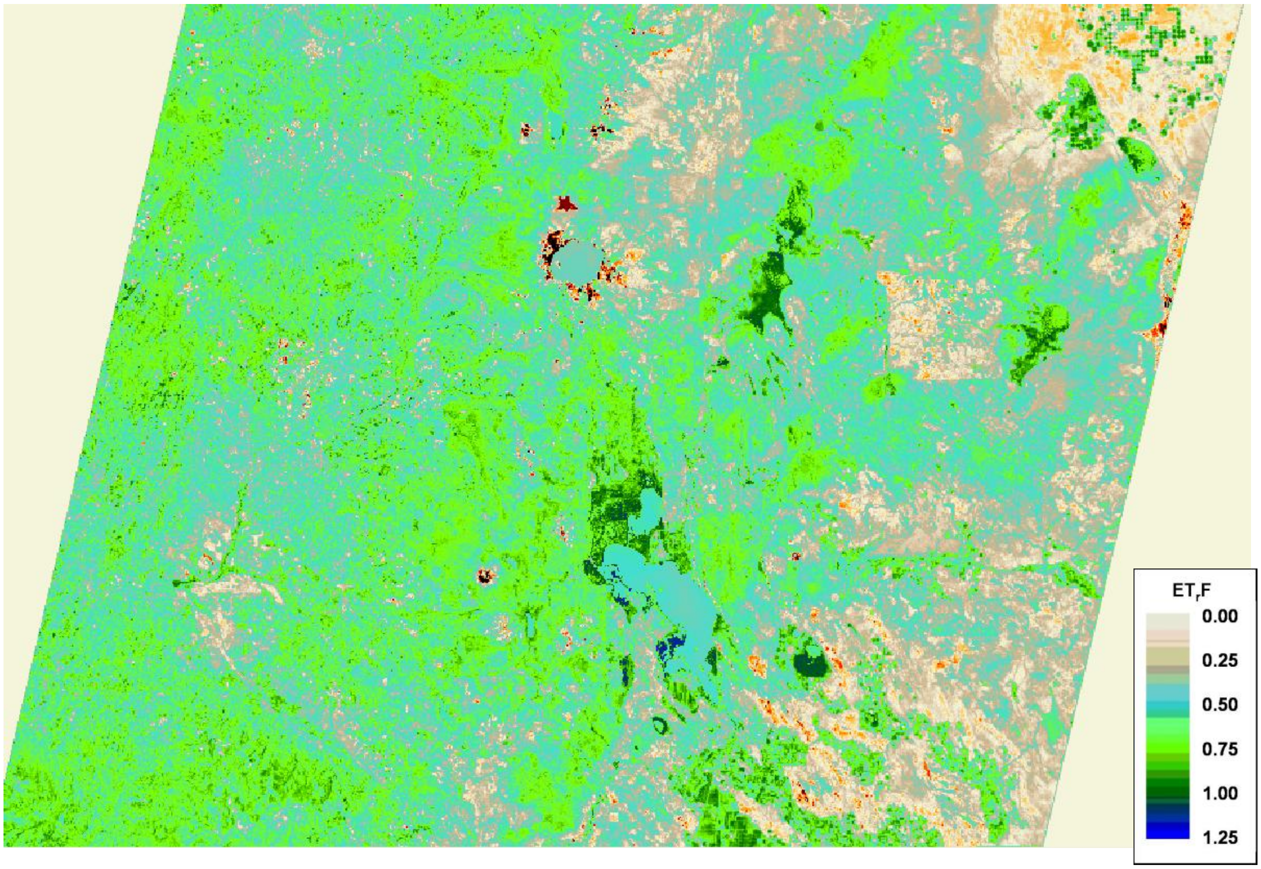

Figure 14. ET$_r$F map for 07/25/2006. Masked cloudy areas are identified as black. Redish spots are negative ET$_r$F values computed during the energy balance process, usually due to complexities in terrain. Negative values are set to 0 during the splining of monthly ET.

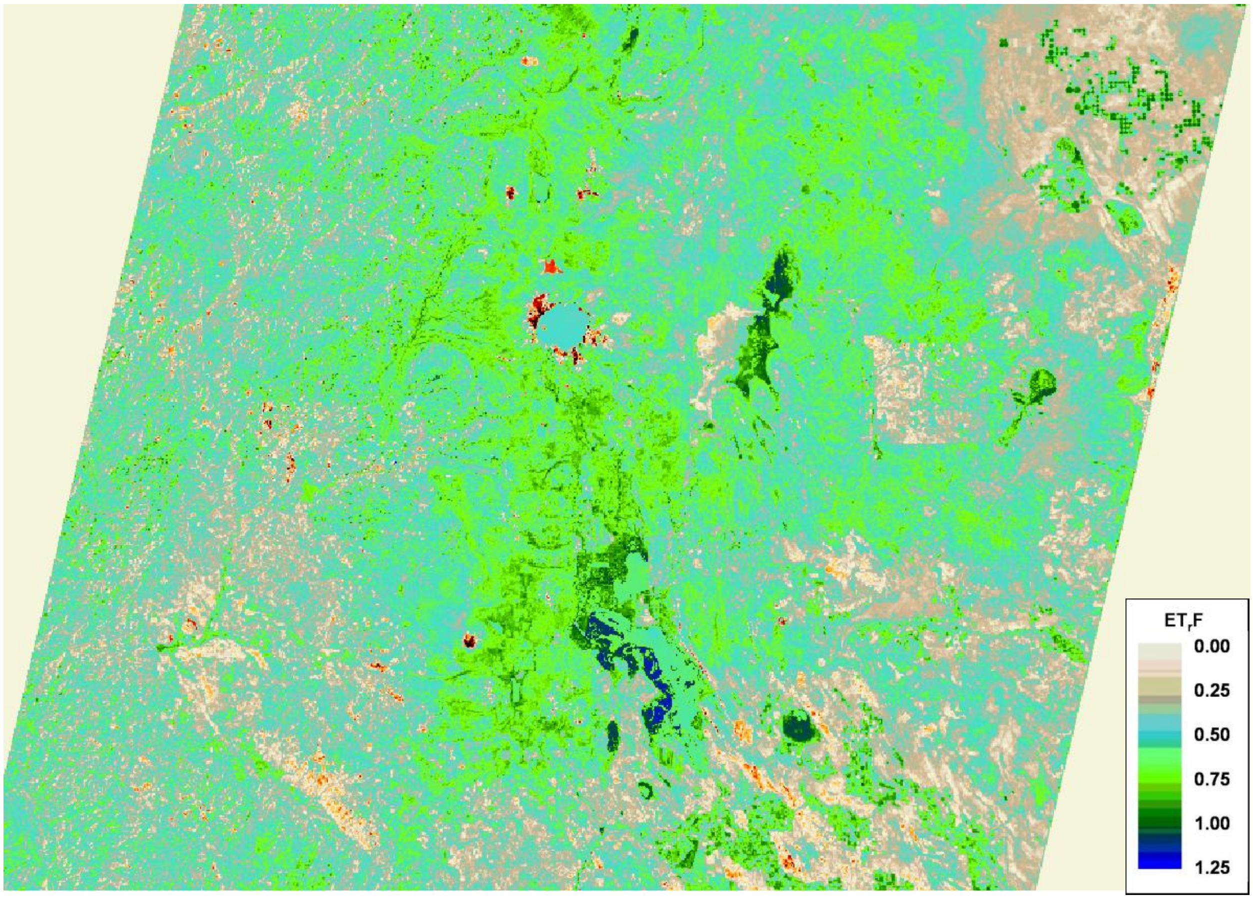

Figure 15. ET$_r$F map for 08/26/2006. Masked cloudy areas are identified as black.

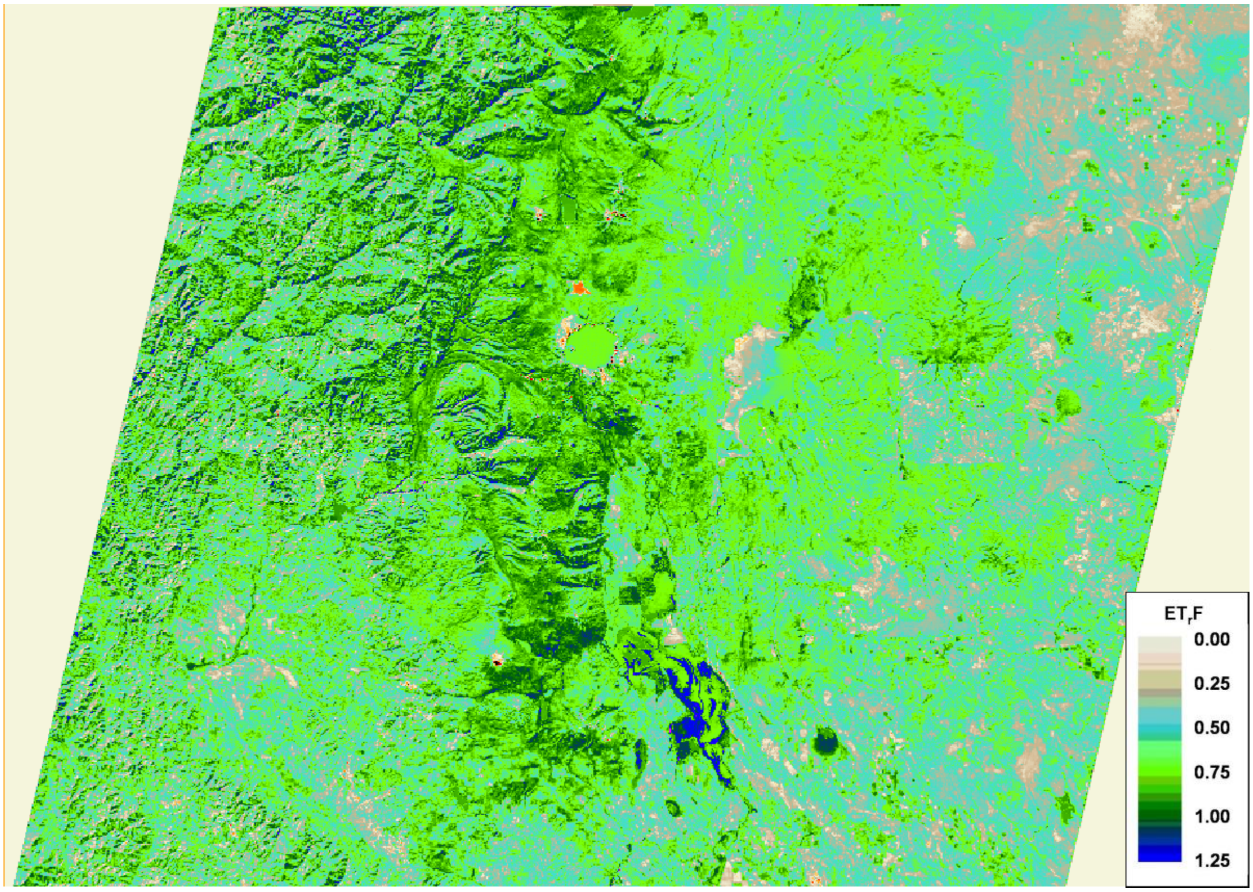

Figure 16. ET_rF map for 09/27/2006. Masked cloudy areas are identified as black.

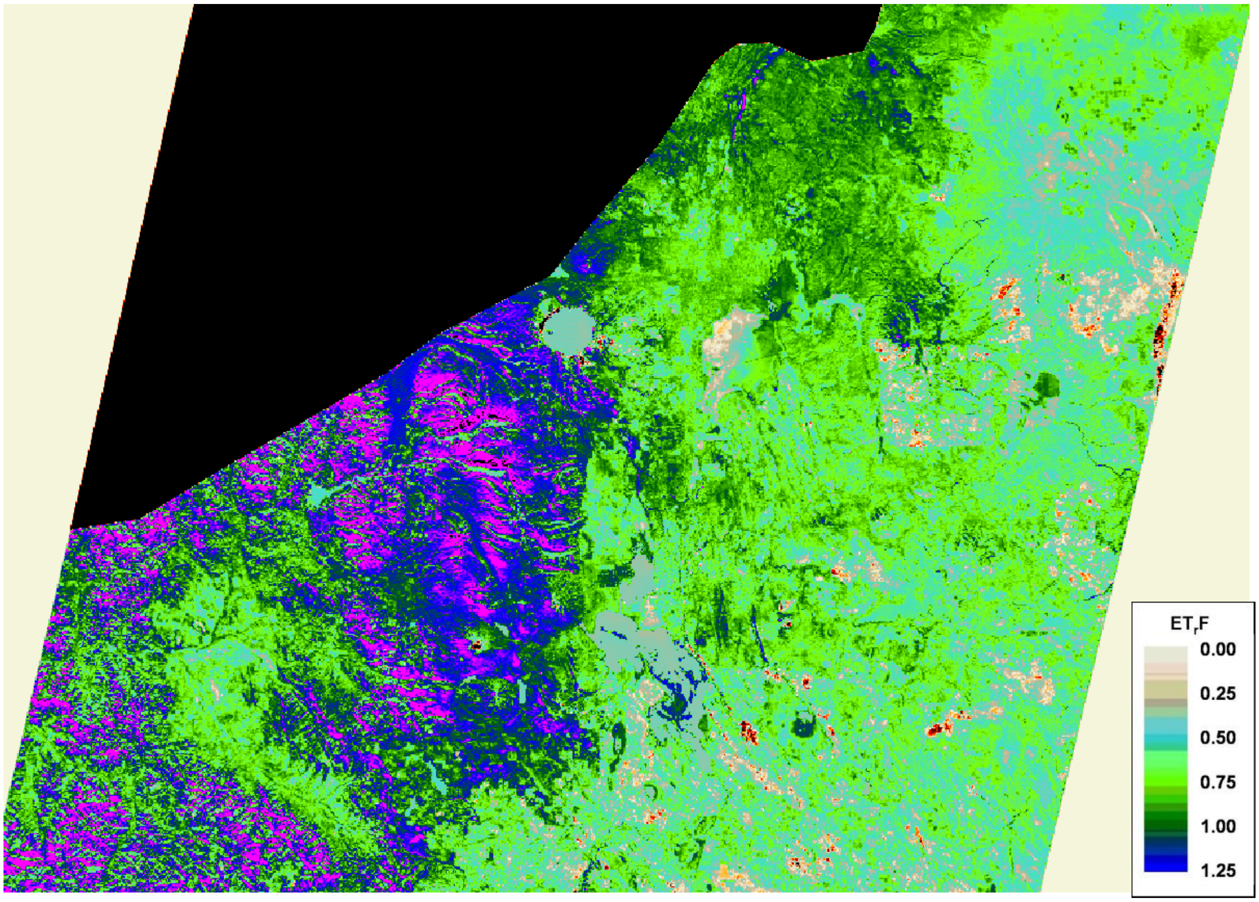

Figure 17 ET_rF map for 10/29/2006. Masked cloudy areas are identified as black. Mountainous regions showed very high values for ET_rF. Some of this was caused by recent rain events in mountain areas. Some of the high values may have been caused by artifacts associated with very cold surface temperatures in mountains due to low sun angles and relatively short time between sunrise and satellite overpass (about 1100 hours) for surface warming. These artifacts are interpreted in the METRIC process as indication of evaporative cooling. The period following the October 29 image was very wet (see Figure 6) so that these high ET_rF values in the mountains may be representative of conditions during that period. In addition, total ET, represented by reference ET (and based on weather) is relatively low during October-November, so that error in ET_rF during this period has less impact on total growing season ET. The resulting monthly ET_rF product (Figure 26) had lower values for ET_rF due to influence of the September 27 image.

Monthly ET and ET_rF

Individual satellite images are processed using METRIC and yield daily maps of ET_rF for the image dates only. ET_rF changes with time between images as vegetation develops or matures or as surface water availability varies. Because the objective of METRIC applications is to produce monthly and seasonal ET based on the information provided by the individual images, ET_rF information from individual satellite image dates is interpolated between image dates to follow the trends caused by vegetation development and evaporation from precipitation. These interpolated, daily ET_rF values are then multiplied by daily reference ET for each day to account for impacts of weather on potential ET demand. These products (of ET_rF x ETr) are then summed over monthly periods to produce monthly ET.

Cubic spline interpolation of ET_rF values between satellite dates

METRIC uses a cubic spline interpolation method to describe a smoothed variation in ET_rF between images. This methodology was found to work better than a simple linear interpolation. For illustration of the cubic spline interpolation method, the figure 18 below shows an example (from another region) of point values of ET_rF sampled from a single pixel from multiple images processed using METRIC. In this figure, values for each image date are connected using linear line segments between image dates.

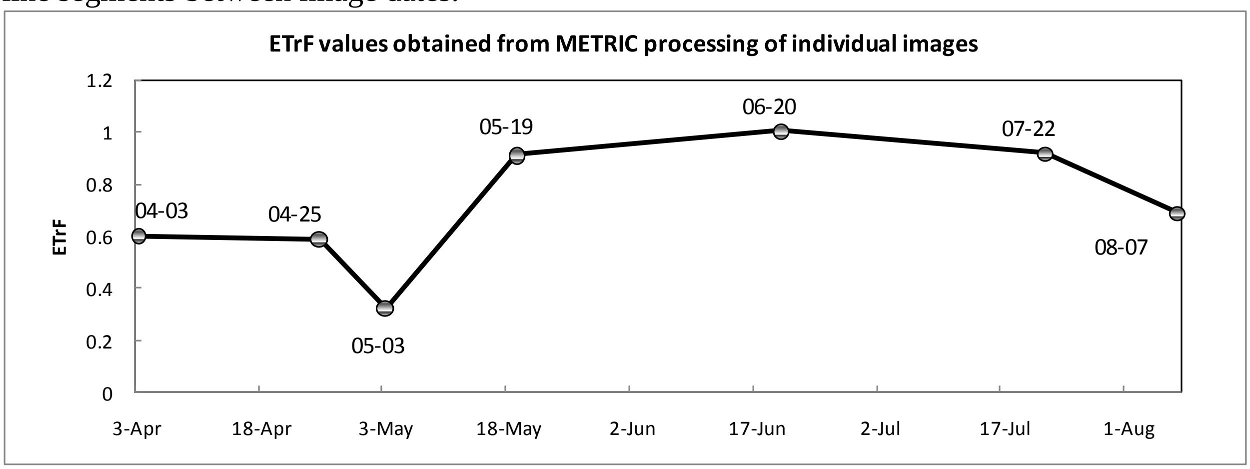

Figure 18. Interpolated ET_rF using linear interpolation between images dates.

Relatively abrupt changes in slope occur between dates. Figure 19 shows the application of a spline interpolation method for the same image dates. This smoother interpolation is in most cases a better representation the development of ET_rF for vegetation compared to the linear interpolation.

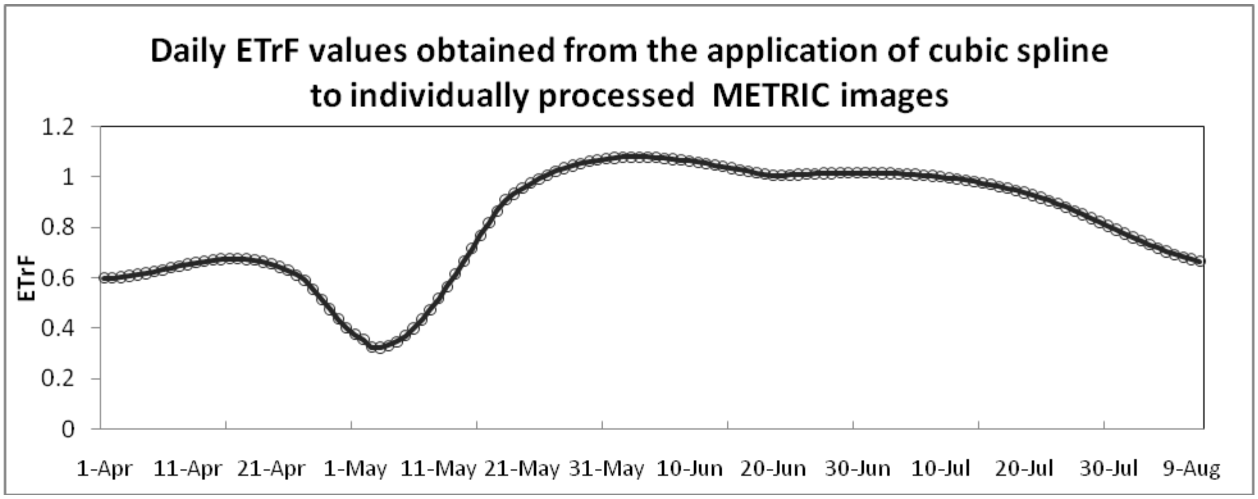

Figure 19. Interpolated ET_rF using cubic spline interpolation between images dates.

The application of the cubic spline procedure to derive monthly and seasonal ET_rF and ET is applied one month at a time. Once the daily images for ET_rF for each day of the month are created, for each day, the ET_rF for every pixel in an image is multiplied by the reference ET (ET_r), computed for each specific day according to weather data:

$$ET_{daily} = ET_rF_{daily} \text{ x } ET_{r\ daily}$$

Following the computation of daily ET for each day of the month, the ET_{daily} was summed to produce ET_{month}. The average monthly ET_rF_{month} was then determined by dividing the ET_{month} by the summed $ET_{r\ month}$:

$$ET_rF_{month} = ET_{month} / ET_{r\ month}$$

Because ET_r can change spatially within an image domain, an inverse distance interpolation procedure of Arc-GIS with standard default parameters was used to produce a daily ET_r surface using twelve Agrimet weather stations to create daily maps of ET_r. The resolution of the daily ET_r images was coarser than that for ET_rF, since ET_r changes only gradually in space. Location information for the Agrimet stations is listed in Table 3. Description of some stations is provided in Appendix A.

Once ET and ET_rF images for all months (April through October) were produced, the same concept as above was applied for the generation of the seasonal images, by summing the monthly ET and dividing by summed ET_r to generate the average seasonal ET_rF.

As such the final generated products were the monthly ET and ET_rF images from April through October and the seasonal total ET and average ET_rF images for both considered paths. All ET_rF images were generated as a Float Single Data Type and the ET images were generated as 16-bit Signed data type previously rounded to avoid data truncation.

Table 3. Agrimet stations used to calculate daily reference ET during 2004 and 2006, including daily ET_r surfaces for use during splining and integrating METRIC ET over monthly periods.

Station	State	Latitude, dec.	Longitude, dec.	Latitude	Longitude	Elevation, ft
Christmas_Valley	OR	43.24139	120.728	43° 14' 29"	120° 43' 41"	4305
Agency_Lake	OR	42.56528	121.983	42° 33' 55"	121° 58' 57"	4150
Beatty	OR	42.47806	121.274	42° 28' 41"	121° 16' 26"	4320
Lakeview	OR	42.12222	120.523	42° 07' 20"	120° 31' 23"	4770
Lorella	OR	42.07778	121.224	42° 04' 40"	121° 13' 27"	4160
Klamath_Falls	OR	42.16472	121.755	42° 09' 53"	121° 45' 18"	4100
Worden	OR	42.0125	121.788	42° 00' 45"	121° 47' 15"	4080
Medford	OR	42.33111	122.938	42° 19' 52"	122° 56' 16"	1340
Cedarville	CA	41.58528	120.171	41° 35' 07"	120° 10' 17"	4600
Powell_Butte	OR	44.24833	-120.95	44° 14' 54"	120° 56' 59"	3200
Hills_Creek_Dam	OR	43.70972	122.421	43° 42' 35"	122° 25' 17"	1560
Lookout_Point_Dam	OR	43.91556	122.752	43° 54' 56"	122° 45' 08"	940

Dealing with clouded parts of images

Satellite images often have clouds in portions of the images, and the Path 45 images of Oregon for years 2004 and 2006 were no exception. ET_rF cannot be directly estimated for clouded areas using surface energy balance because cloud temperature masks surface temperature and cloud albedo masks surface albedo. ET_rF for clouded areas must be filled in before splining of monthly ET. Because clouded (or 'missing') portions of an image generally result in long periods between valid ET_rF data (sometimes longer than several months), a special cloud-filling procedure was used.

ET_rF for cloud masked areas is filled in for individual Landsat dates prior to splining ET_rF between images. The ET_rF data inserted into masked areas are 'borrowed' from adjacent images in time, but with adjustment for background evaporation occurring from precipitation events, and, in some cases, adjusting total ET_rF to account for substantial changes in image-wide vegetation amounts, for example during early spring. The adjustment for background evaporation is made in proportion to the amount of exposed bare soil in a pixel. The latter is estimated in proportion to 1/NDVI, where NDVI is the normalized difference vegetation index. The impact of the adjustment for background evaporation during cloud-filling is more seamless agreement between filled and adjacent nonfilled areas. The cloud mask-gap filling and interpolation of ET between image dates entails interpolating the ET_rF for the missing area from the previous and following images.

An ERDAS Imagine Modelmaker code was created by the University of Idaho METRIC group to conduct the 'filling' of cloud masked portions of images. The procedure is explained in details in Appendix 19 of the METRIC manual (Allen et al, 2010).

Results of monthly ET_rF maps

Figures 20 to 26 show monthly ET_rF maps for the period between April and October 2006 that were produced using cloud-filled images for individual dates and splining ET_rF between dates.

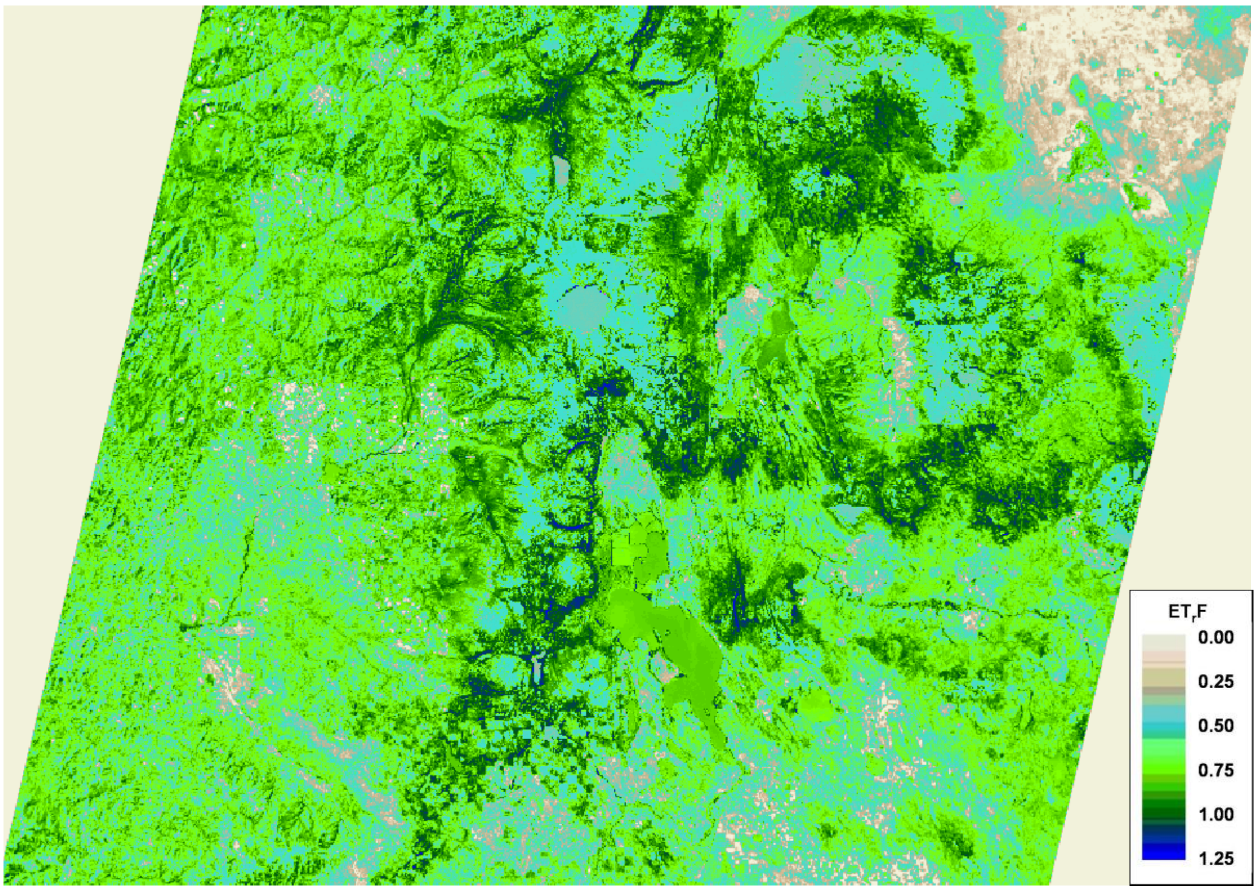

Figure 20. Average ET_rF map for April 2006

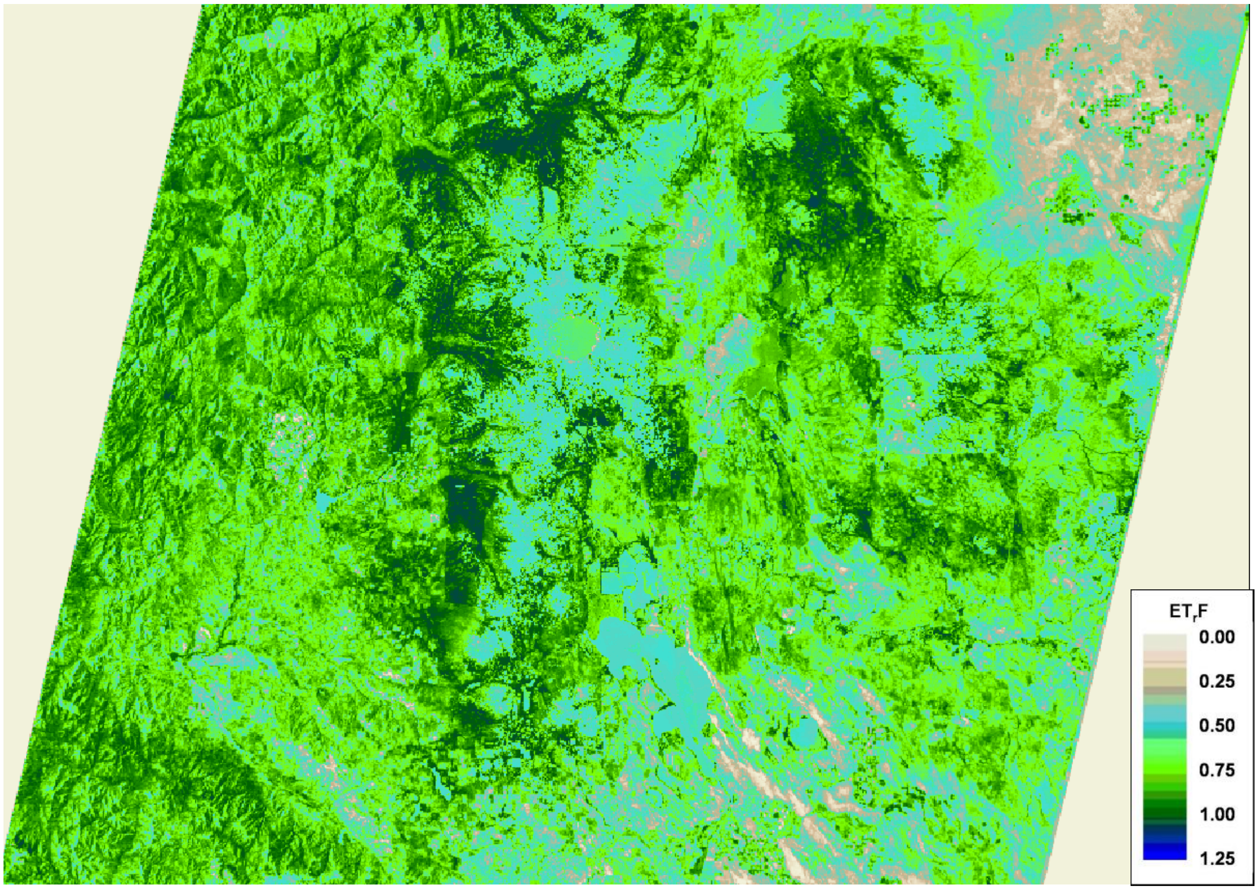

Figure 21. Average ET_rF map for May 2006

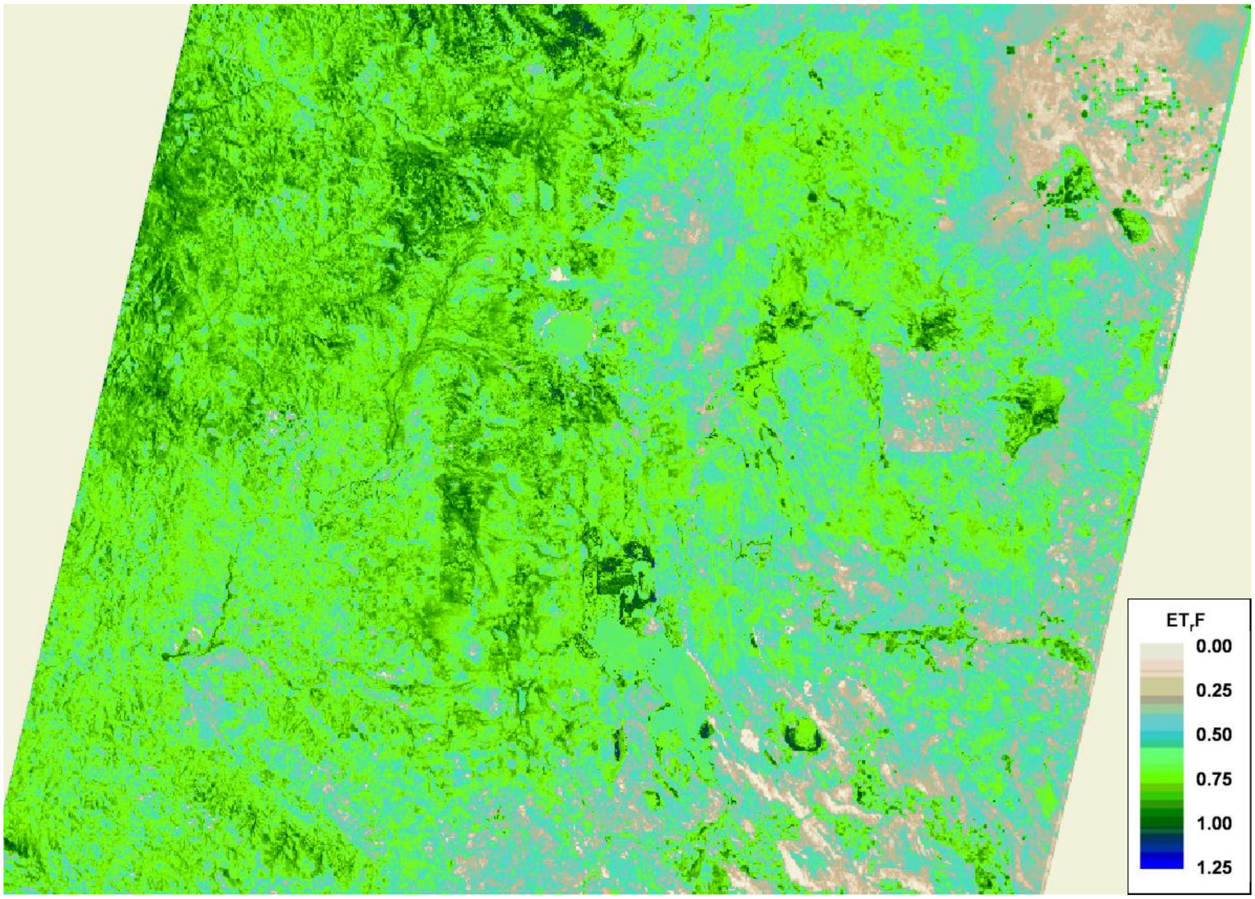

Figure 22. Average ET$_r$F map for June 2006

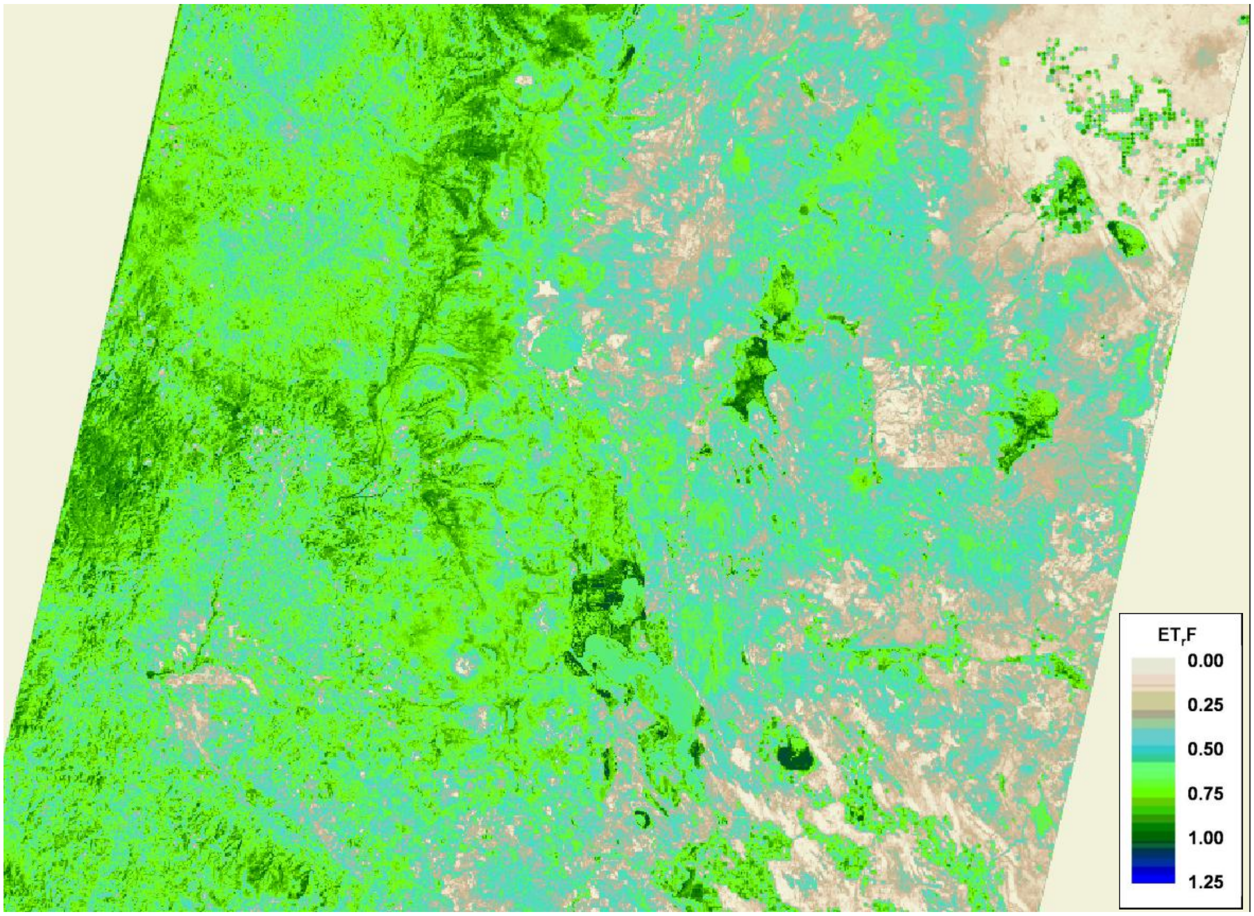

Figure 23. Average ET$_r$F map for July 2006

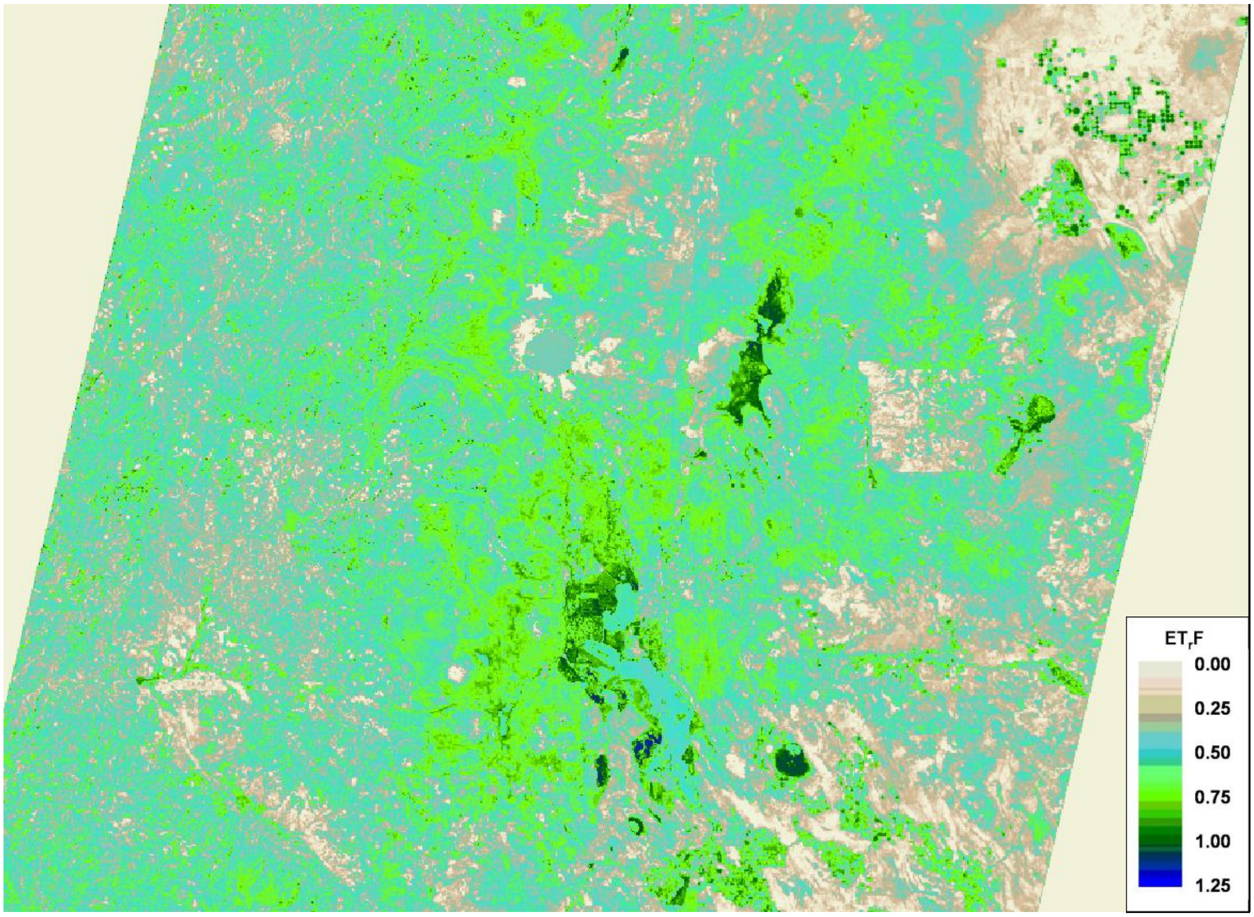

Figure 24. Average ET$_r$F map for August 2006

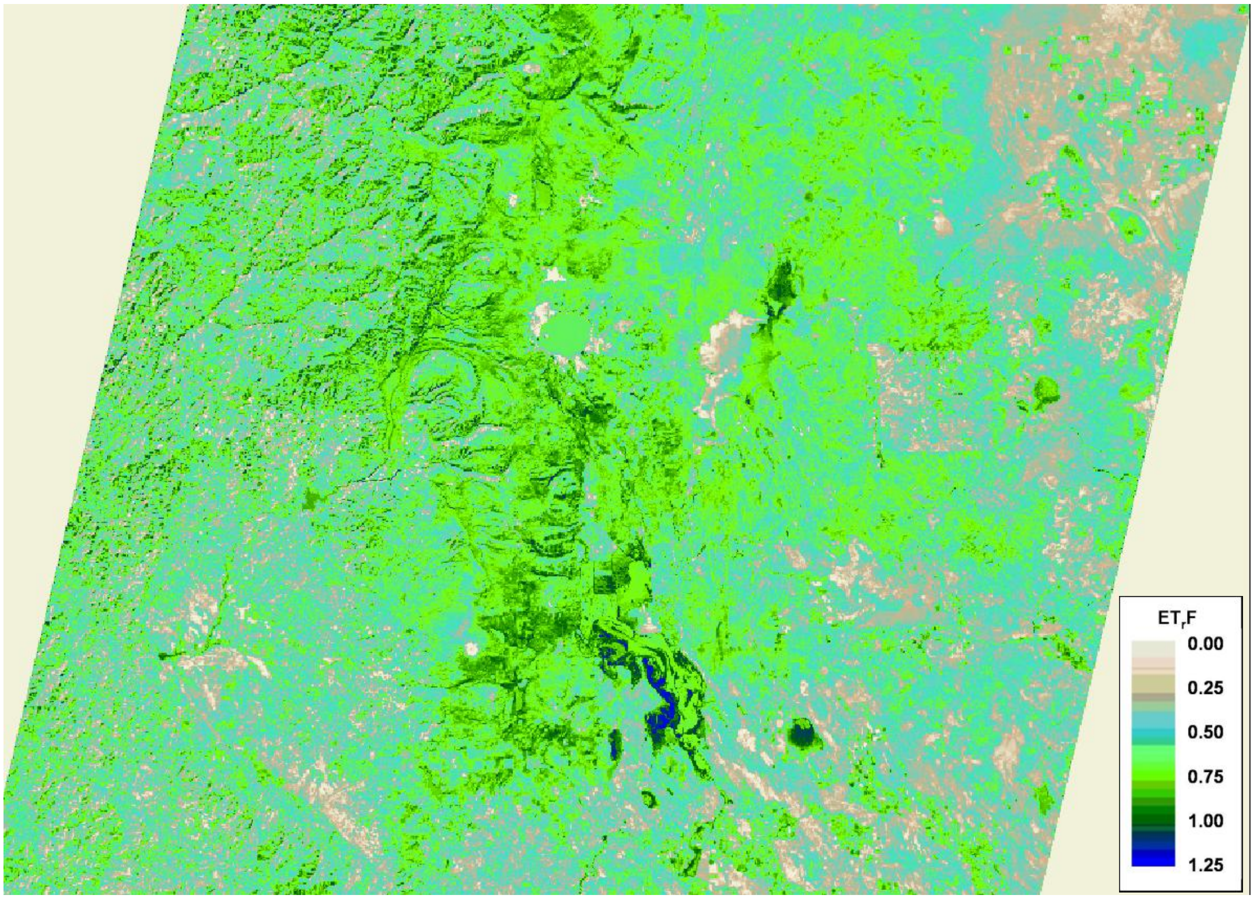

Figure 25. Average ET_rF map for September 2006

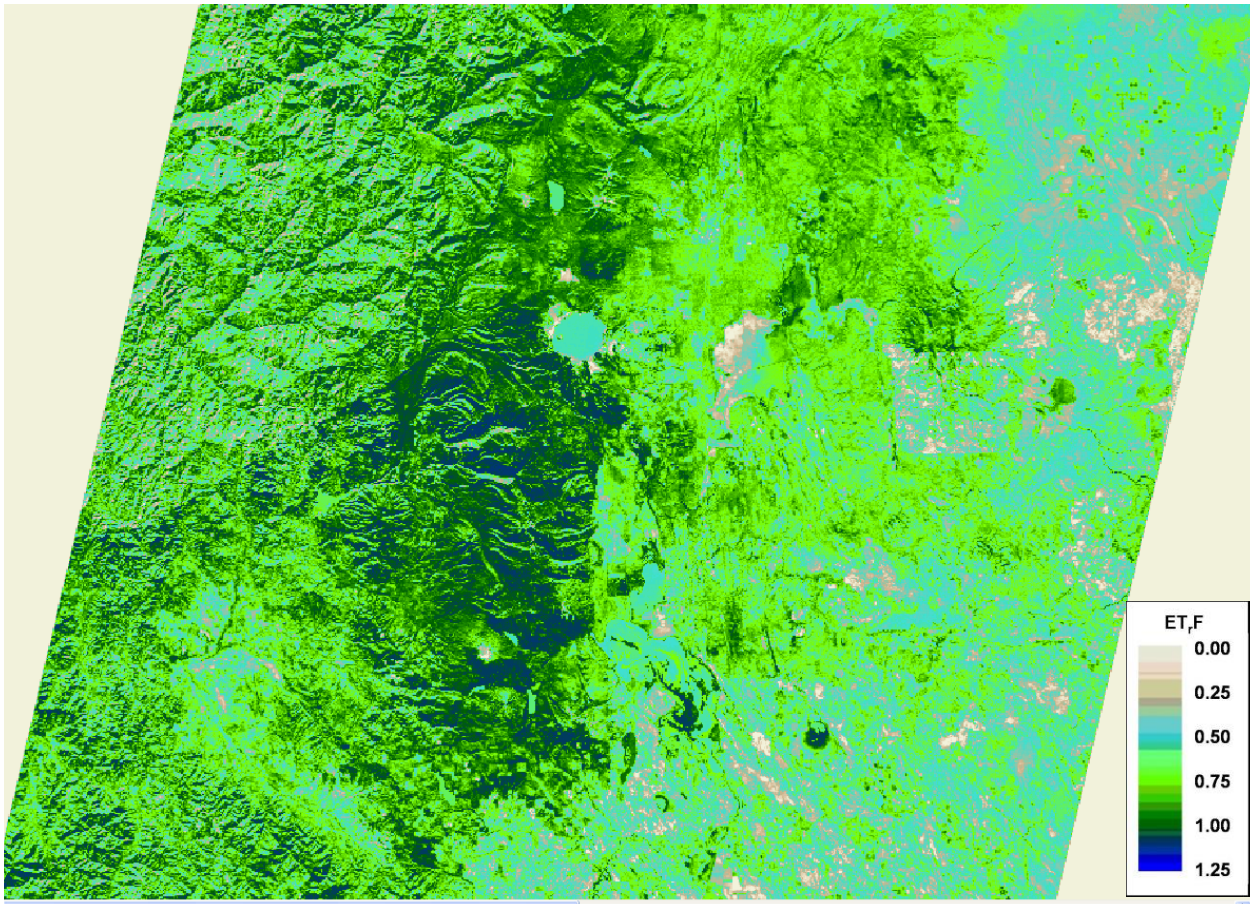

Figure 26. Average ET_rF map for October 2006

Seasonal ET and ET_rF

Seasonal ET from April to October 2006 was calculated by summing ET from each month. Finally an average ET_rF map was generated by dividing the seasonal ET by the total ET_r for the same period. The average seasonal ET_rF map is shown in Figure 27. A close up of seasonal ET_rF is shown in Figure 28 for the Sprague River area and in Figure 29 for the Klamath Falls area.

Total ET from nonirrigated areas, as computed by the METRIC process, was generally in the range of annual precipitation. Table 4 is a summary of ranges of ET estimated from METRIC for nonirrigated areas near noted weather station locations. April-October 2006 ET is compared to precipitation from January-December, 2006. The annual period was summed to consider winter precipitation that may have been stored in soil and carried into the growing season. ET ranged considerably with land use type and aspect, as well as probable soil types and depths. Some error may exist in both growing season ET and precipitation, with the former occurring during temporal interpolation between satellite images and the latter occurring from spatial interpolation of point measurements.

Table 4. Ranges of ET estimated from METRIC for nonirrigated areas near noted locations during 2006, where ET is likely to be from precipitation, only (no shallow ground-water, wetlands, etc)

Location	General ET range, mm during April-October	Precipitation, mm during January-December
Christmas Valley	100 - 240	170
Mountains in NW Image	600 - 900	---
Timbered areas west of Crater Lake	700 - 1000	---
West of Agency Lake	300 - 600	400
Upper Sprague basin	100 - 300	260 (Lorella)
South of Klamath	70 - 400	310

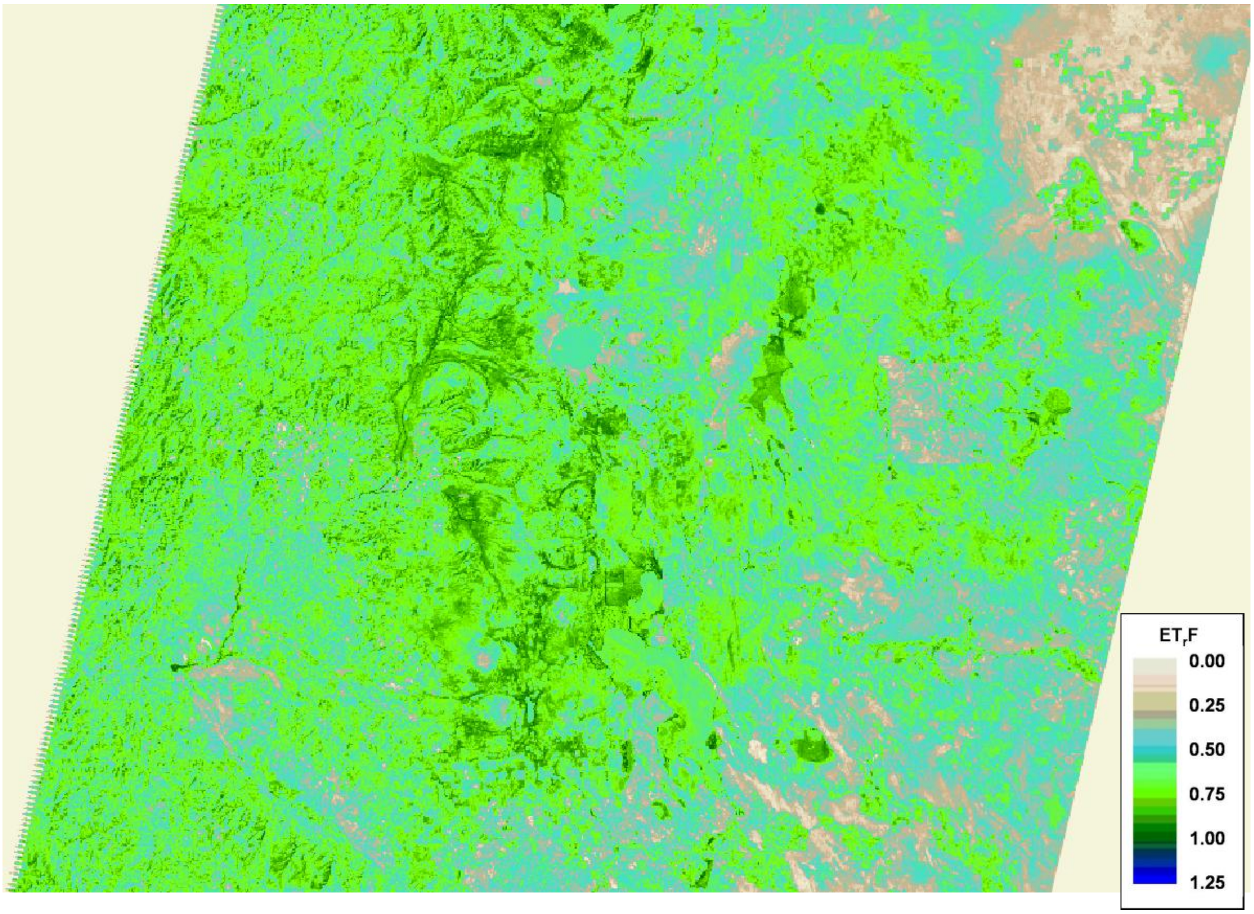

Figure 27. Average seasonal ET$_r$F map for the period between April to October 2006

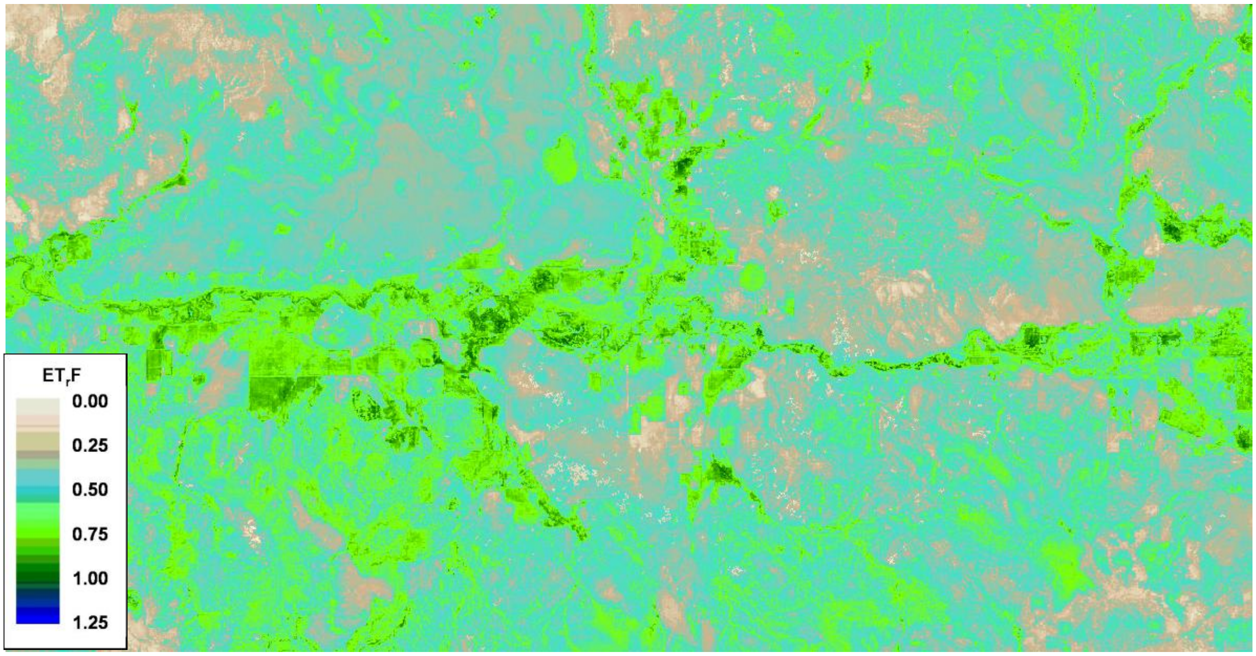

Fig. 28. Close up of average seasonal ET_rF for the period April-October in the Sprague River area for 2006.

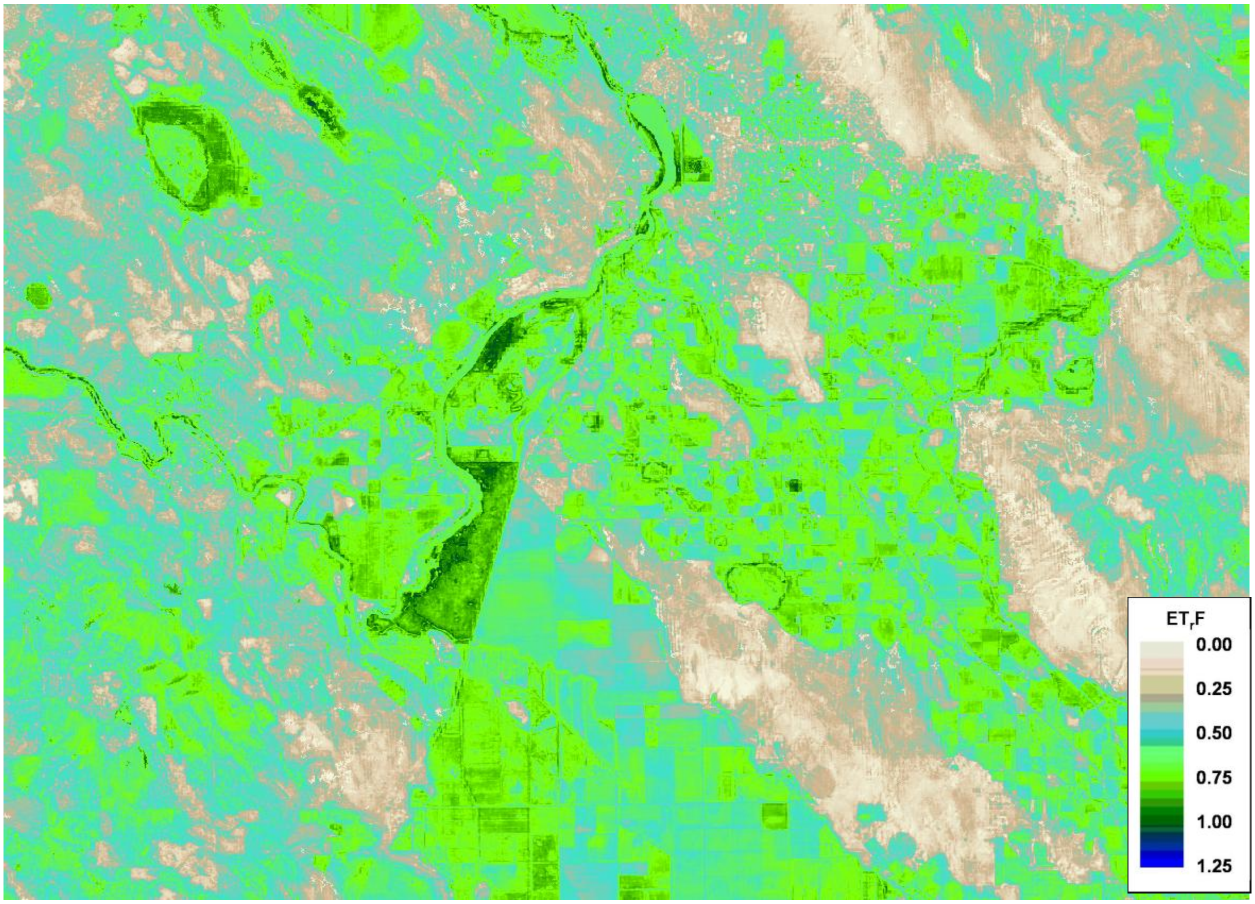

Fig. 29. Close up of average seasonal ET$_r$F for the period April-October near Klamath Falls, 2006.

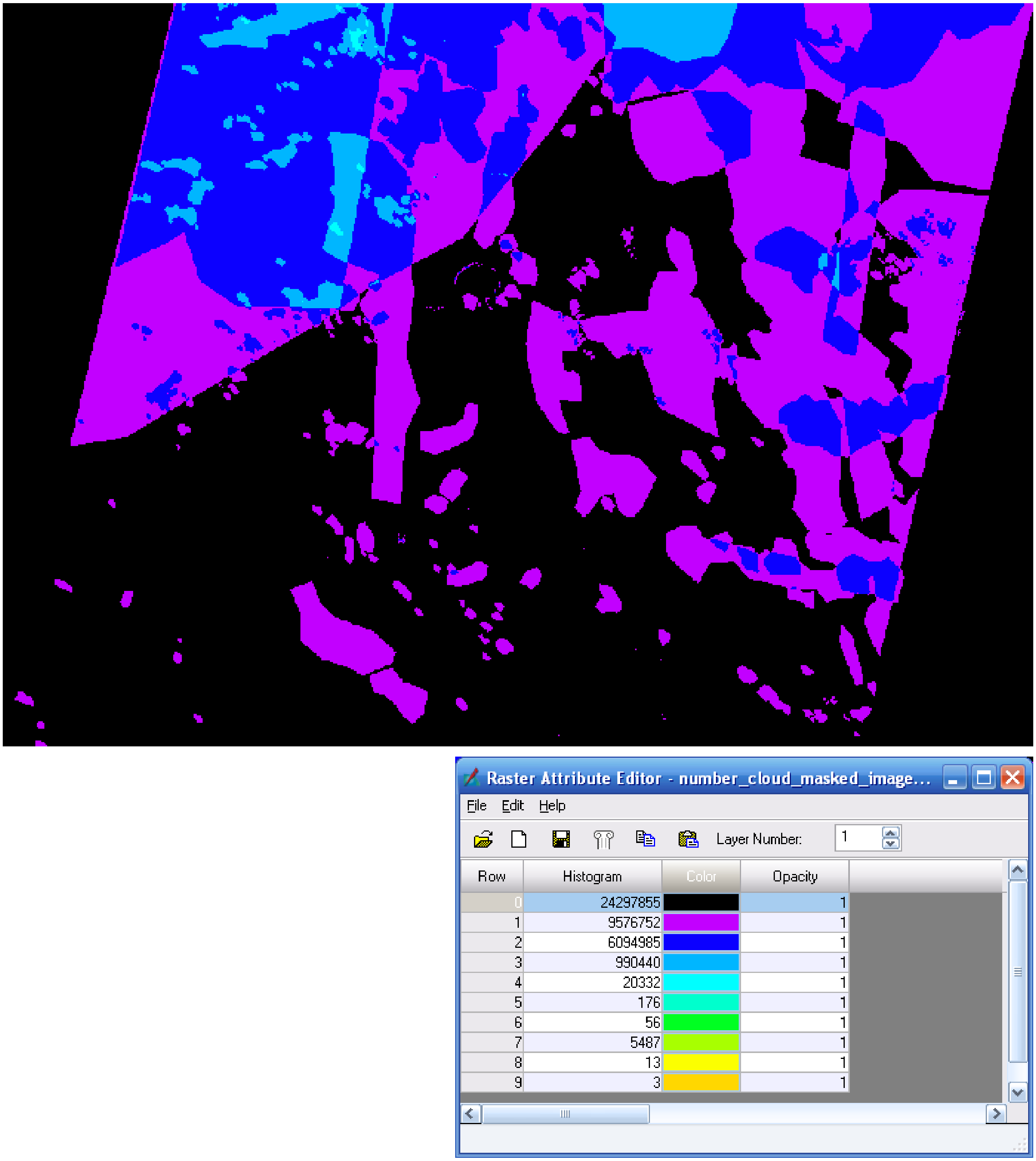

Row	Histogram	Color	Opacity
0	24297855		1
1	9576752		1
2	6094985		1
3	990440		1
4	20332		1
5	176		1
6	56		1
7	5487		1
8	13		1
9	3		1

Fig. 30. Number of clouded images as part of the 9-image-based seasonal ET product for 2006. Black = 0, magenta = 1, dark blue = 2, light blue = 3 (see legend below the image).

7. References

Allen, R.G., 2008. REF-ET: Reference Evapotranspiration Calculation Software for FAO and ASCE Standardized Equations. University of Idaho, 82 pp. [http://www.kimberly.uidaho.edu/ref-et/index.html]. Contact author for updates.

Allen, R.G., Pereira, L.S., Raes, D., Smith, M., 1998. Crop Evapotranspiration. Guidelines for computing crop water requirements. FAO Irrigation and Drainage Paper 56. FAO, Rome, 300 pp. http://www.kimberly.uidaho.edu/water/fao56/

Allen, R.G., Pereira, L.S., Smith, M., Raes, D., Wright, J.L., 2005. FAO-56 Dual Crop Coefficient Method for Estimating Evaporation from Soil and Application Extensions. J. Irrig. Drain. Engr., 131(1), 2-13. http://ddr.nal.usda.gov/bitstream/10113/39505/1/IND43693971.pdf

Allen, R.G., Tasumi, M., Morse, A., Trezza, R., Wright, J.L., Bastiaanssen, W., Kramber, W., Lorite, I., Robison, C.W., 2007a. Satellite-Based Energy Balance for Mapping Evapotranspiration with Internalized Calibration (METRIC) – Applications. J. Irrig. Drain Engr., 133(4), 395-406. http://www.kimberly.uidaho.edu/water/papers/remote/ASCE_JIDE_Allen_et_al_METRIC_application2007_QIR000395.pdf

Allen, R.G., Tasumi, M., Trezza, R., 2007b. Satellite-Based Energy Balance for Mapping Evapotranspiration with Internalized Calibration (METRIC) – Model. J. Irrig. Drain Engr., 133(4), 380-394. http://www.kimberly.uidaho.edu/water/papers/remote/ASCE_JIDE_Allen_et_al_METRIC_model_2007_application2007_QIR00380.pdf

Allen, R.G., Tasumi, M., Trezza, R., Kjaersgaard, J.H., 2010. METRIC. Mapping Evapotranspiration at High Resolution. Applications Manual, V 2.0.4. University of Idaho. 166 pp.

ASCE-EWRI, 2005. The ASCE Standardized Reference Evapotranspiration Equation. ASCE, Reston, Virginia. http://irrisoftet/downloads/literature/ASCE Standardized_Equation Jan 2005.pdf

Trezza, R., Allen, R.G., Robison, C.W., Kramber, W.J., Kjaersgaard, J., Tasumi, M., Garcia, M., 2008. Enhanced Resolution of Evapotranspiration from Riparian Systems and Field Edges by Sharpening the Landsat Thermal Band. Paper presented at the 2008 World and Environmental Resources Congress of ASCE and EWRI, Honolulu, HI, May 12-16, 2008. Published on CD-ROM, ASCE. 12 p.

Wright, J.L., 1982. New evapotranspiration crop coefficients. J. Irrig. Drain. Engr., 108(1), 57-74. http://eprints/nwisrl.ars.usda.gov/382/478.pdf

Appendix A. Descriptions of weather stations within the project area

On November 13 - 16, 2010, Rick Allen, Ricardo Trezza and Eric Kra toured the upper Klamath and Sprague River basins to review general land-use and agricultural production conditions and to review Agrimet weather stations. Of the 12 Agrimet stations used to estimate reference ET_r (Table A-1 below), the Klamath Falls, Beatty, Lakeview, Lorella and Medford stations were visited. We were unable to reach the Agency Lake site due to locked access.

Table A-1. Agrimet stations used to calculate daily reference ET during 2004 and 2006, including daily ET_r surfaces for use during splining and integrating METRIC ET over monthly periods.

Station	State	Latitude, dec.	Longitude, dec.	Latitude	Longitude	Elevation, ft
Christmas_Valley	OR	43.24139	120.728	43° 14' 29"	120° 43' 41"	4305
Agency_Lake	OR	42.56528	121.983	42° 33' 55"	121° 58' 57"	4150
Beatty	OR	42.47806	121.274	42° 28' 41"	121° 16' 26"	4320
Lakeview	OR	42.12222	120.523	42° 07' 20"	120° 31' 23"	4770
Lorella	OR	42.07778	121.224	42° 04' 40"	121° 13' 27"	4160
Klamath_Falls	OR	42.16472	121.755	42° 09' 53"	121° 45' 18"	4100
Worden	OR	42.0125	121.788	42° 00' 45"	121° 47' 15"	4080
Medford	OR	42.33111	122.938	42° 19' 52"	122° 56' 16"	1340
Cedarville	CA	41.58528	120.171	41° 35' 07"	120° 10' 17"	4600
Powell_Butte	OR	44.24833	-120.95	44° 14' 54"	120° 56' 59"	3200
Hills_Creek_Dam	OR	43.70972	122.421	43° 42' 35"	122° 25' 17"	1560
Lookout_Point_Dam	OR	43.91556	122.752	43° 54' 56"	122° 45' 08"	940

Klamath Falls Agrimet

The Klamath Falls Agrimet weather station is located at the Oregon State University Research Center south of Klamath Falls. The area is mostly agricultural with some residential and industrial development. Windbreaks to the south and west of the station may impact air flow at times, as might proximity of research buildings to the weather station.

Klamath Falls Agrimet from the hiway, looking SW

Closeup of Klamath Falls Agrimet looking SW.

Lakeview Agrimet

The Lakeview Agrimet station is located near two center pivots and north of an irrigated cemetery. The very local landcover is dry grass, however, fetch is predominately irrigated.

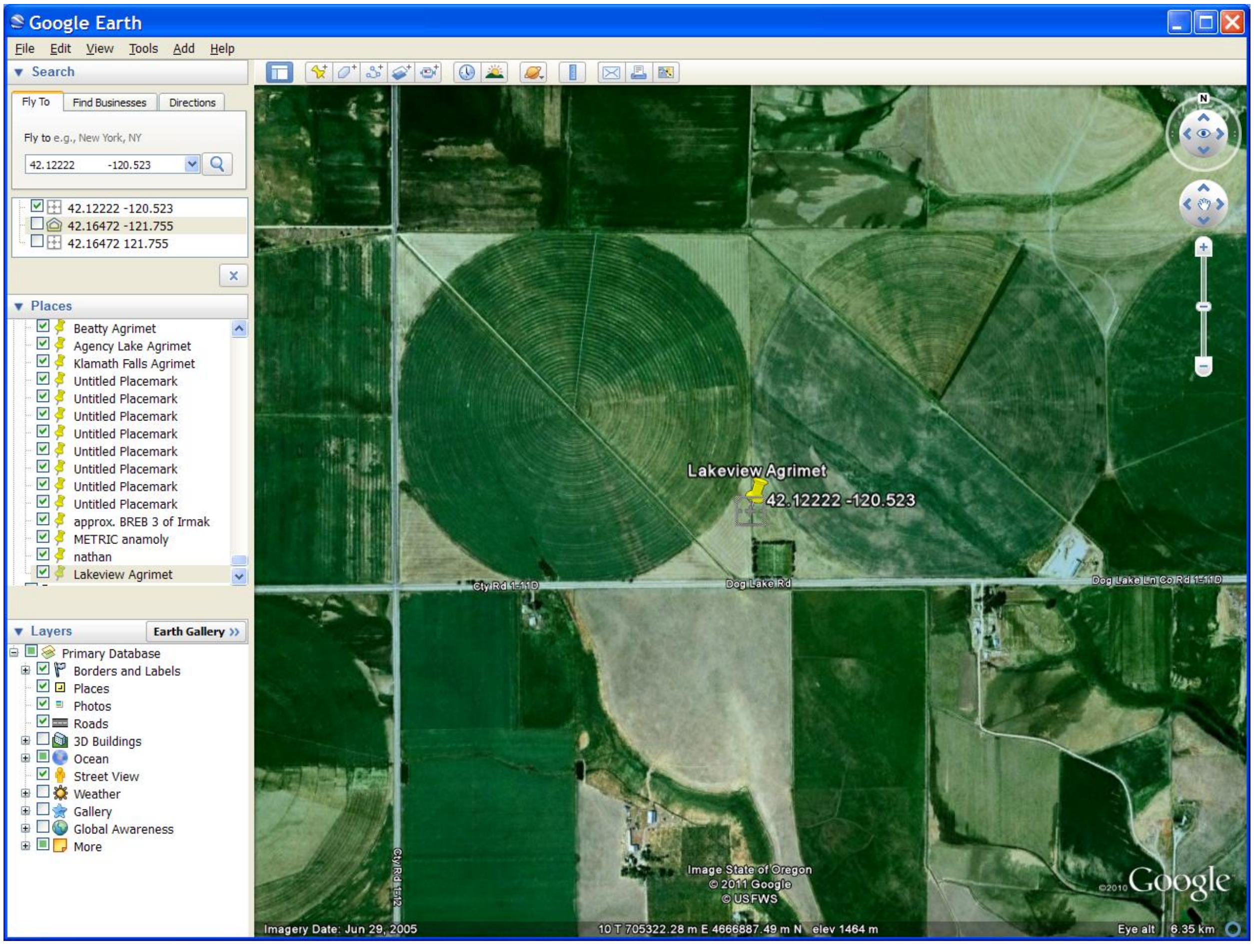

Lakeview Agrimet looking NW

Lakeview Agrimet looking NW, with Allen

Closeup of Lakeview Agrimet station

Medford Agrimet Station

The Medford Agrimet station is located at the Oregon State University Research Center west of Medford. The area is partially agricultural with some residential and industrial development. The station itself is located just north of research buildings and just north of a small grapevine study. The area to the north and east is mostly open. The buildings to the south and the grapevines probably impact air flow at times. It would be helpful on all Agrimet stations if anemometers were set at 3 m height above ground rather than the current 2 m height.

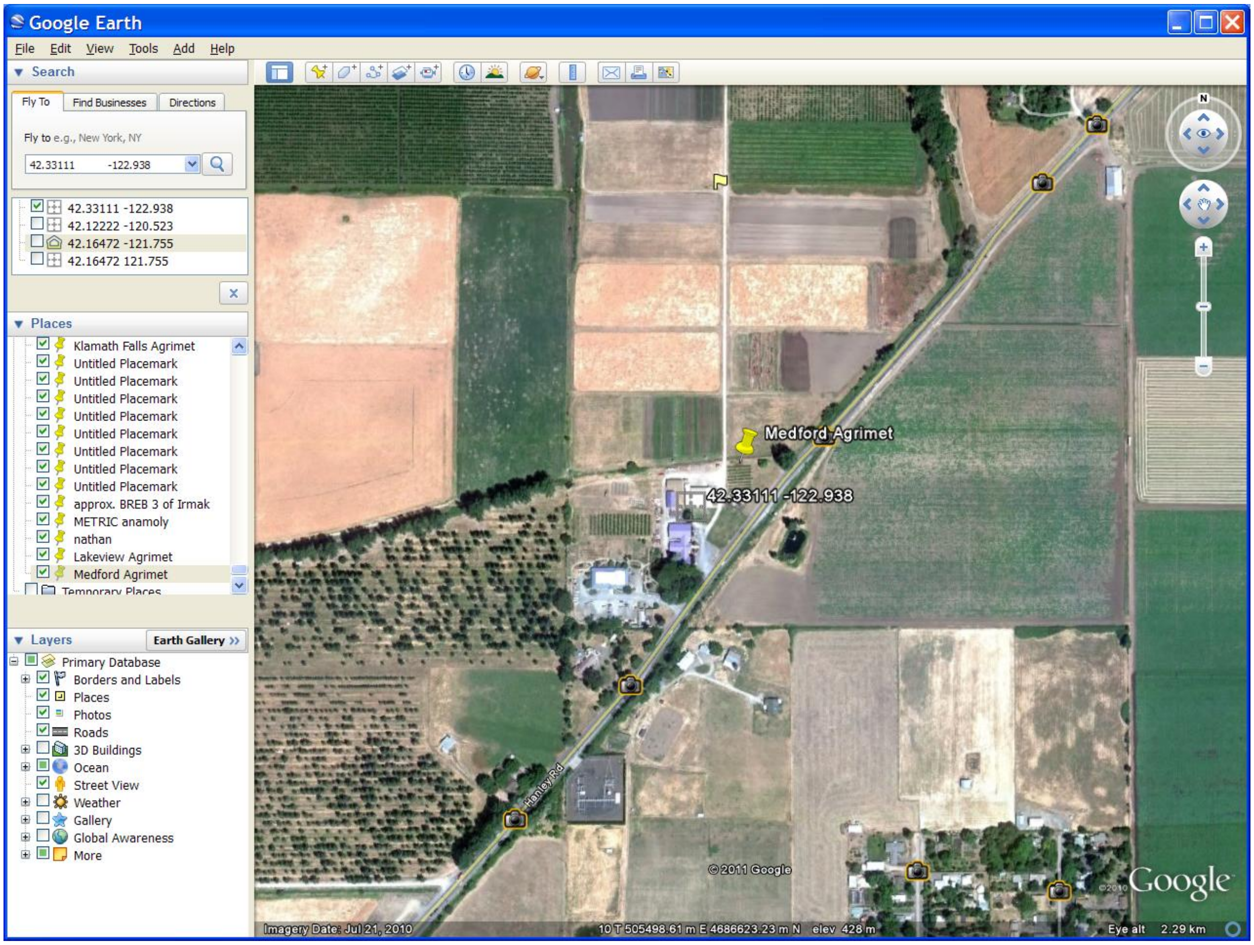

Medford Agrimet station with Trezza and Allen

Medford Agrimet Station looking East

Medford Agrimet Station looking North.

Appendix B. Generation of Precipitation and Reference ET_r surfaces

Daily precipitation surfaces were created using precipitation (P) information from 45 COOP stations and 7 Agrimet stations located within and adjacent to the scene processed. Data for COOP stations were downloaded from the NOAA National Climatic Data Center (NCDC) web site. Agrimet data were obtained from the USBR Agrimet web site. A shapefile indicating the COOP and Agrimet station locations was created and is available. The locations of the stations for precipitation are shown in the following figure B1.

An Inverse Distance Weighting function was used for the interpolation of P and ETr, which can create some discontinuities and some 'bulls eyes' around stations having higher or lower readings as compared to surrounding stations (figure B2). This is mostly an artifact from the interpolation method. Towards the center of the image is Crater Lake, where there is a COOP station on the mountain (Crater Lake is a lake inside a volcano) and the mountain receives substantially more P as compared to the surrounding areas.

The ET_r surfaces are based on 9 (2004) or 10 (2006) Agrimet weather stations. We used a spline interpolation for the ET_r surfaces where we increased the tension setting in Arc to 10 to prevent the spline from increasing ET_r beyond reasonable values for areas in between weather stations. The process created an ERDAS file for each day of 2004 and 2006, and stacks by month and the seasonal sum, all in units of mm.

The COOP station P data were adjusted for the time-of-day (usually 7 am) of readings, so that if the precipitation was recorded before noon, we moved the data to the previous day, while if the precip was recorded after noon, we did not move it. For this reason, there is sometimes a one day 'shift' in precip between nearby stations, so that one station may have recorded say 10 mm one day and nothing on the next, while a neighboring station is the opposite. Later, in the process of adjusting the image date ET_rF from METRIC for background evaporation, we therefore typically take the average of three days when estimating what the ET_rF was at the satellite overpass date. The P surfaces have one file for each day of 2004 and 2006, and stacks by month and the seasonal sum, all in units of mm. At this point, the gridded precipitation data have not been used. They were assembled in case a gridded evaporation process model would have been needed to estimate total evaporation over monthly periods from bare soil conditions, to use to adjust Landsat images for background evaporation differences between image dates and surrounding monthly periods. However, review of ET data from METRIC did not indicate the need to make this adjustment. STATSGO soil maps for Oregon and California, and the derived water content at 15 bars and 1/3 bar, available water capacity and soil texture for Oregon in were assembled, but again, not required. Other input to the soil water balance model, including TEW (total evaporable water), REW (relative extractable water), De_initial and P_eff_to_D_initial, were computed.

The following two figures (figs. B2 and B3) show gridded precipitation summed over January – December 2006 for an area slightly larger than the processed image area and gridded reference ET summed for the April – October 2006 period for the nearly the same area.

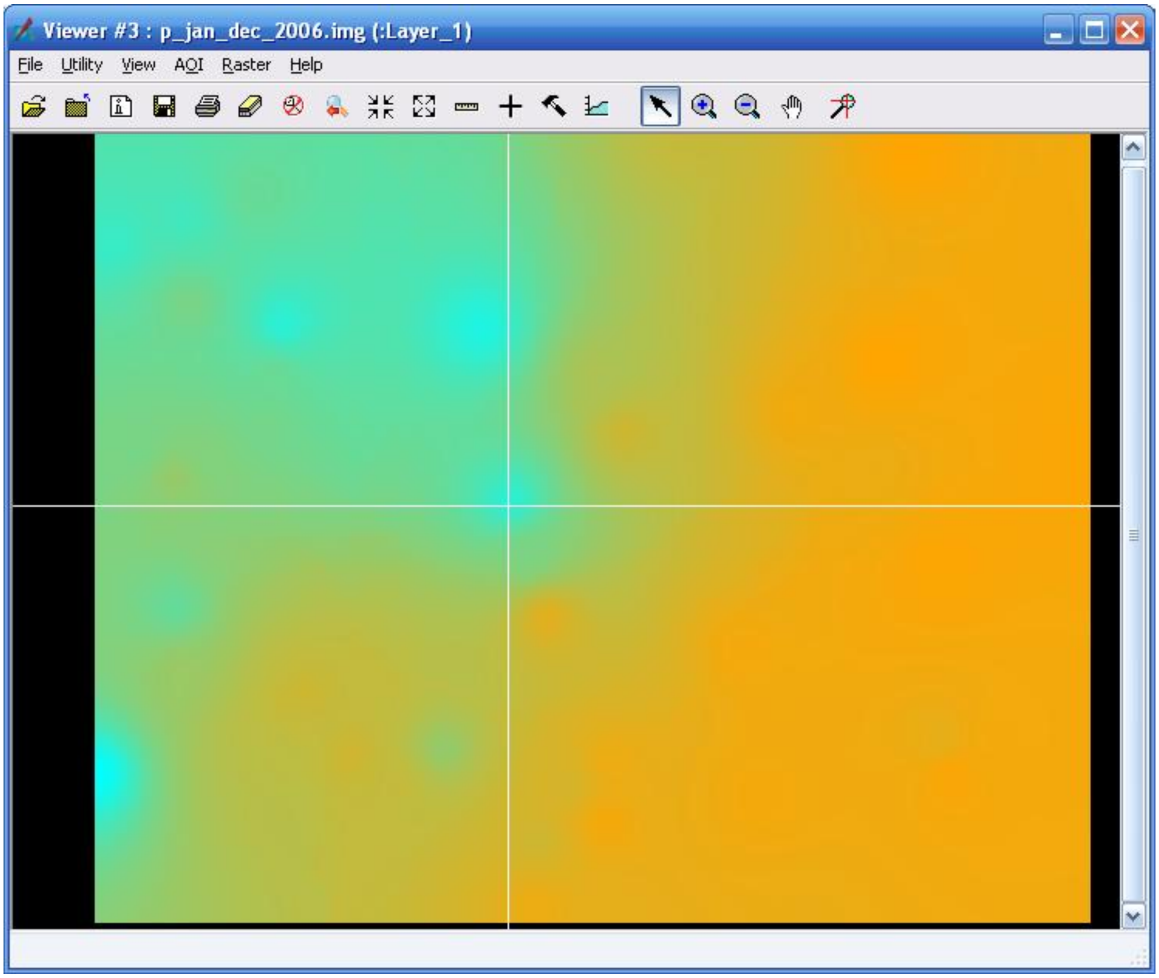

Fig. B2. Interpolation of total January – December, 2006 precipitation over the study area, with orange at 200 mm to blue at 1800 mm. The cross hair is centered over Crater Lake.

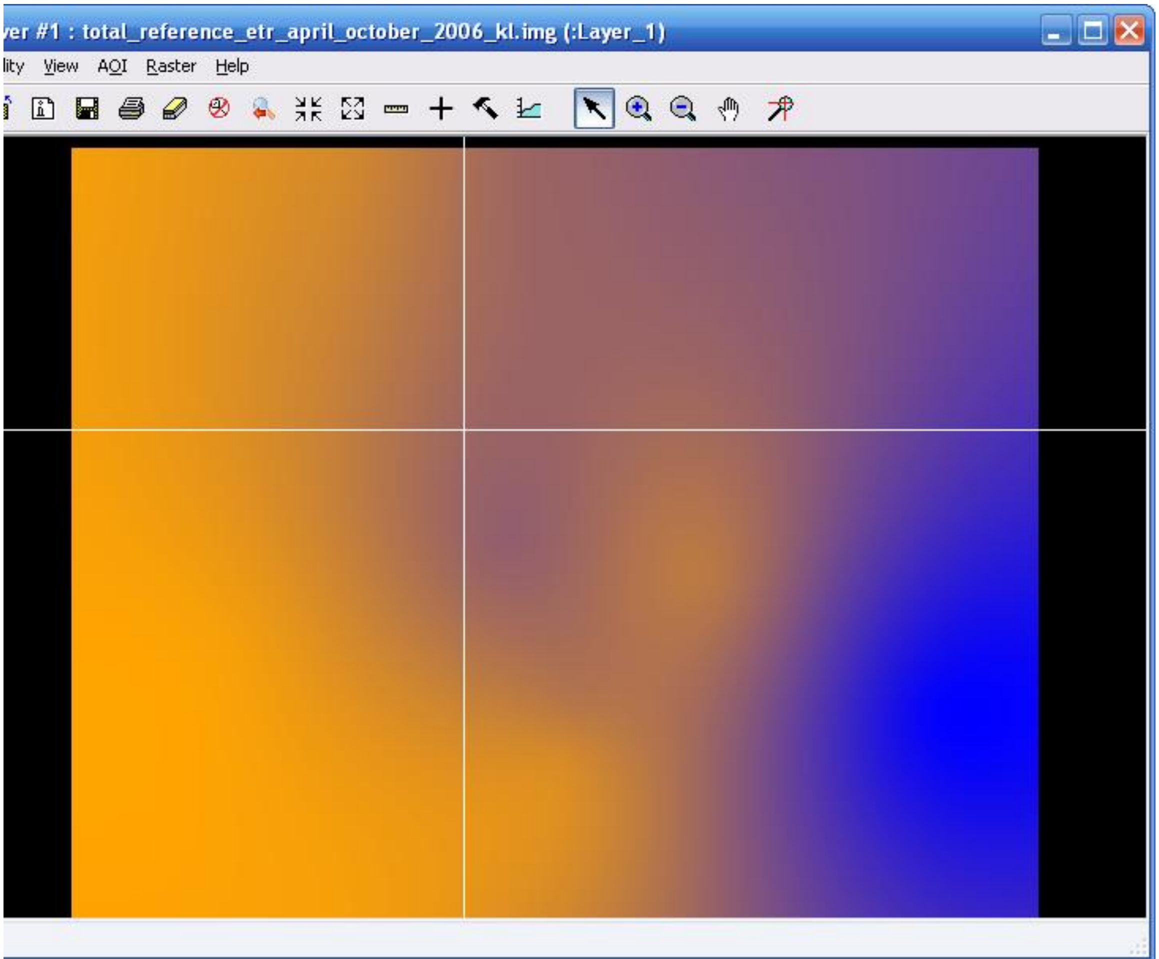

Fig. B3. Interpolation of total Alfalfa reference ET_r from April to October, 2006 over the study area, with orange at 980 mm to blue at 1250 mm. The cross hair is centered over Crater Lake.

Appendix C. Description of Products contained in this Drive for METRIC processing for Klamath, Oregon, Year 2006

All spatial data files are presented in ERDAS Imagine data format (*.img). This format is a raster format that can contain multiple layers. Data are generally in 'float' (real) value expressions (including all images using mm depths and all ET_rF), but some are expressed in integer form (DEM). The Imagine formatted files are readily read by all modern Arc-GIS systems. For some images, including the monthly ET and ET_rF files, the data have been 'colorized' to display in ERDAS imagine in color. This helps with visualization to the person viewing the data, but do not impact the data themselves. The colorization may not transfer into the Arc-GIS system. The colorization is viewed in ERDAS by opening the files in 'pseudo color' mode. Each "img" file is accompanied by an 'rrd' file that is generated by ERDAS to facilitate rapid zooming and statistics. The rrd files are not important to Arc-GIS usage.

Primary Folder Klamath_2006_path_45:

SubFolder: 2006_path_45_original_Landsat_images_trimmed_to_Klamath

This folder contains the original Landsat images(8 bit digital numbers (0-255)) used during METRIC processing. Each image is comprised of seven layers, where Layer 1 = Landsat Band 1; Layer 2 = Landsat Band 2; Layer 3 = Landsat Band 3; Layer 4 = Landsat Band 4; Layer 5 = Landsat Band 5; Layer 6 = Landsat Band 6 (thermal band); Layer 7 = Landsat Band 7.

Image Name	Units	Description
l71045030_03120060428_klamath.img	DN	Landsat 7 image corresponding to 04/28/2006
l5045030_03120060506_klamath.img	DN	Landsat 5 image corresponding to 05/06/2006
l71045030_03120060530_klamath.img	DN	Landsat 7 image corresponding to 05/30/2006
l5045030_03120060623_klamath.img	DN	Landsat 5 image corresponding to 06/23/2006
l5045030_03120060709_klamath.img	DN	Landsat 5 image corresponding to 07/09/2006
l5045030_03120060725_klamath.img	DN	Landsat 5 image corresponding to 07/25/2006
l5045030_03120060826_klamath.img	DN	Landsat 5 image corresponding to 08/26/2006
l5045030_03120060927_klamath.img	DN	Landsat 5 image corresponding to 09/27/2006
l5045030_03120061029_klamath.img	DN	Landsat 5 image corresponding to 10/29/2006

The naming convention is "L1t" = level 1, terrain corrected, followed by MMDDYYYY for the date, followed by the path and center row, followed by the satellite type (Landsat 5 or 7).
All of the images correspond to Landsat WRS path 45, comprised mainly of row 30, plus some portions of row 31 residing north of the Oregon-California state line, as shown in the following figure. Spatial resolution of pixels is 30 m for all bands. However, original resolution of Landsat 5 band 6 (the thermal band) was 120 m and of Landsat 7 was 60 m. These bands were resampled, however, using cubic convolution, by the USGS EROS data center prior to dissemination.

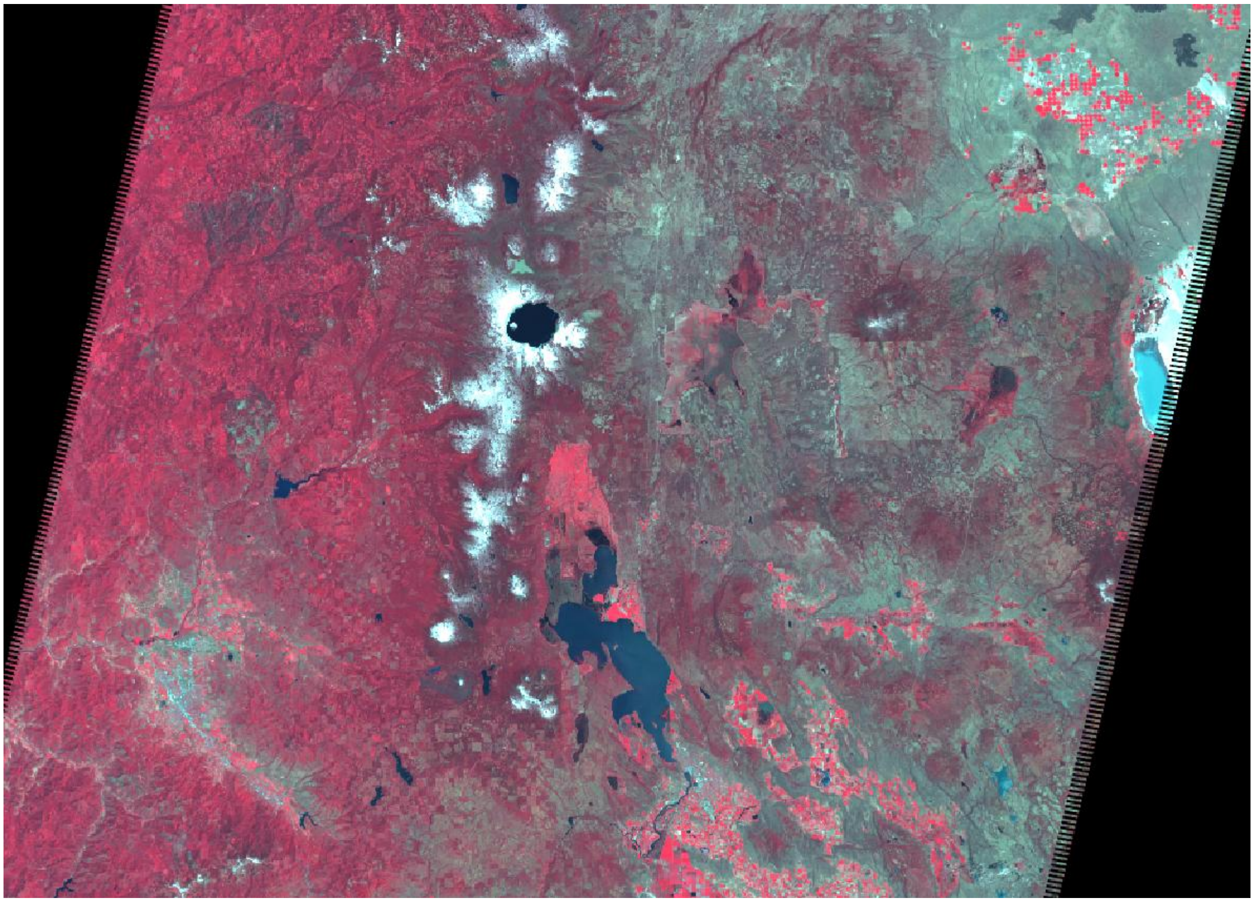

The following table shows the seven bands and their wavelength range from each satellite.

Band Number	Original resolution (m)	Landsat 5 wavelength (µm)	Landsat 7 wavelength (µm)
B1 (blue)	30	0.452 – 0.518	0.452 – 0.514
B2 (green)	30	0.528 – 0.609	0.519 – 0.601
B3 (red)	30	0.626 – 0.693	0.631 – 0.692
B4 (NIR)	30	0.776 – 0.904	0.772 – 0.898
B5 (MIR)	30	1.567 – 1.784	1.547 – 1.748
B6 (thermal,TIR)	60 (LS7), 120 (LS5)	10.45 – 12.42	10.31 – 12.36
B7 (MIR)	30	2.097 – 2.349	2.065 – 2.346
B8 (panchromatic)*	10 (LS7 only)	NA	0.515 – 0.896

*Not used for ET and ET_rF map generation.

SubFolder: 2006_path_45_landuse map

This folder contains the landuse map used for METRIC processing. The map was derived from the USGS NLCD (National Land Cover Database) Land Use map, and it was downloaded from the USGS-seamless webpage (http://seamless.usgs.gov/). The NLCD map is primarily used during determination of aerodynamic roughness values.

Image Name	**Description**
landuse_p45r30_31.img	Land use map

SubFolder: 2006_path_45_DEM

This folder contains the DEM map used for METRIC processing. The map was downloaded from the USGS-seamless webpage (http://seamless.usgs.gov/) and has 30 m resolution.

Image Name	**Description**
dem_combined_reproj.img	Map of pixel elevation, in meters, combined for paths 44 and 45.

Folder: 2006_path_45_cloudmasked_ETrF_on_image_date

This folder contains the daily images produced from METRIC and represents the ET estimate for each Landsat image date. The pixel values represent the ratio (ET_rF) between actual evapotranspiration (ET) and alfalfa-reference evapotranspiration (ETr). A value of ET_rF =0.6 means that ET is 60% of ET_r. "Black" areas in these images are areas that were 'cloud masked' to delete those areas that were impacted by cloud cover.

Image Name	**Units**	**Description: $ET_rF = ET/ ET_r$**
etrf24_cloudmasked_04282006_p45r30_l7_klamath.img	fraction	ET_rF image corresponding to 04/28/2006
etrf24_cloudmasked_05062006_p45r30_l5_klamath_color.img	fraction	ET_rF image corresponding to 05/06/2006
etrf24_cloudmasked_05302006_p45r30_l7_klamath.img	fraction	ET_rF image corresponding to 05/30/2006
etrf24_cloudmasked_06232006_p45r30_l5_klamath_color.img	fraction	ET_rF image corresponding to 06/23/2006
etrf24_cloudmasked_07092006_p45r30_l5_klamath_color.img	fraction	ET_rF image corresponding to 07/09/2006

etrf24_cloudmasked_07252006_p45r30_l5_klamath_color.img	fraction	ET_rF image corresponding to 07/25/2006
etrf24_cloudmasked_08262006_p45r30_l5_klamath_color.img	fraction	ET_rF image corresponding to 08/26/2006
etrf24_cloudmasked_09272006_p45r30_l5_klamath_color.img	fraction	ET_rF image corresponding to 09/27/2006
etrf24_cloudmasked_10292006_p45r30_l5_klamath_color.img	fraction	ET_rF image corresponding to 10/29/2006

The naming convention is ETrF24 followed by the date expressed as MMDDYYYY, followed by the path row and satellite number. The image named number_cloud_masked_images_p45r30_klamath_2006.img shows the number of images that were clouded for any particular location during the 2006 growing season (see Figure 30 in the main text).

Folder: 2006_path_45_monthly_et_maps

This folder contains the monthly ET maps (in millimeters) for every month, from April to October 2006. For example, a pixel value = 120 means that a total 120 mm of ET was calculated for that particular pixel for that particular month.

Image Name	**Units**	**Description**
et_april2006_kl.img	millimeters	Total ET in millimeters for April 2006
et_may2006_kl.img	millimeters	Total ET in millimeters for May 2006
et_june2006_kl.img	millimeters	Total ET in millimeters for June 2006
et_july2006_kl.img	millimeters	Total ET in millimeters for July 2006
et_august2006_kl.img	millimeters	Total ET in millimeters for August 2006
et_september2006_kl.img	millimeters	Total ET in millimeters for September 2006
et_october2006_kl.img	millimeters	Total ET in millimeters for October 2006

Folder: 2006_path_45_monthly_etrf_maps

This folder contains the average ET_rF for every month, from April to October 2006. This average ET_rF was obtained dividing the total ET by the total ET_r for a particular month. The "monthly" average ET_rF" was produced from the image date-specific ET_rF by splining ET_rF between image dates for each day between the images, multiplying by ET_r of each day, summing the ET product over a month to produce the monthly ET in the previous table, and then dividing by monthly summed ET_r to obtain a monthly average ET_rF. ET_r data were calculated using the University of Idaho REF-ET software using meteorological weather parameters from six Agrimet weather stations in the study area following extensive quality assessment/quality control. The standardized ASCE-EWRI (2005) Penman-Monteith reference ET equation for the tall alfalfa reference type was used.

Image Name	**Units**	**Description**
etrf_april2006_kl_color.img	fraction	Average ET_rF for April 2006
etrf_may2006_kl_color.img	fraction	Average ET_rF for May 2006
etrf_june2006_kl_color.img	fraction	Average ET_rF for June 2006
etrf_july2006_kl_color.img	fraction	Average ET_rF for July 2006
etrf_august2006_kl_color.img	fraction	Average ET_rF for August 2006

etrf_september2006_kl_color.img	fraction	Average ET_rF for September 2006
etrf_october2006_kl_1.img	fraction	Average ET_rF for October 2006

Folder: 2006_path_45_seasonal_et_maps

This folder contains the total ET maps (in millimeters) for the period between April to October 2006 for path 45 (that are based on METRIC energy balance).

Image Name	Units	Description
total_et_april_october_2006_kl_color.img	millimeters	Total ET in millimeters for the period between April to October 2006

SubFolder: 2006_path_45_seasonal_etrf_maps

This folder contains the average ET_rF from April to October 2006 for path 45. This average ET_rF was obtained by dividing the total seasonal ET (from April to October) by the total seasonal ET_r (from April to October).

Image Name	Units	Description
average_etrf_april_october_2006_kl_color.img	millimeters	Total ET in millimeters for the period between April to October 2006

SubFolder: 2006_path_45_Cloud_filling_sources

This folder contains on image for each ET_rF date showing which image date (later in time) that ETrF data were taken from to fill gaps for the image being filled.

Image Name	Units	Description
etrf24_cloudfill_source_04282006_p45r30_l7_klamath.img	---	Image no. later in time for data borrowing

Folder: 2006_path_45_monthly_reference_etr_maps

This folder contains the total alfalfa-refence evapotranspiration (ETr) maps for every month in 2006. ET_r is expressed in millimeters. Reference ET results from REF-ET for 2006 were previously provided with the 2004 data sets. The standardized ASCE-EWRI (2005) Penman-Monteith reference ET equation for the tall alfalfa reference type was used.

Appendix D. Algorithms for estimating aerodynamic roughness and wind speed in mountains

Richard G. Allen and Ricardo Trezza

This appendix describes algorithms developed during early 2011 for the University of Idaho METRIC Mountain model to improve estimation of sensible heat transfer, via the METRIC 'dT function' for mountainous regions. Form drag increases in mountains as a result of impacts of bluff body effects of hills and mountains and separation of flow. Usually, a wake region of chaotic flow where pressure deficiency exists occurs on the lees of mountains. Roughness lengths for such complex terrains are thus much larger than the typical vegetative canopy (Hansen 1993). Hansen summarized roughness lengths for steep mountainous areas to range from 0.7 to 3.0 m, whereas typical roughness for forest ranged from about 0.3 to 1.0 m. Garratt (1977) summarized data and modeling by Fiedler and Panofsky (1972) that suggested roughness of mountainous areas to be 2 to 3 times larger than for 'flat' systems. The literature does not have many suggestions on estimating aerodynamics over large areas of mountainous terrain. The following algorithms are relatively simple functions to increase or decrease wind speed according to noted, physical trends experienced on slopes and to increase aerodynamic roughness in complex terrain to follow general observations from literature.

The basic forms are based on intuition of the writers and are intended to provide approximate adjustments. The nature and shape of the functions and the values for coefficients were determined by making multiple runs of METRIC over mountainous areas of the Klamath watershed in Landsat path 45, row 30 over various times of the year and noting the formulations that produced estimates of ET on a variety of slopes and aspects and for a range of vegetation amounts that were in line with precipitation inputs.

Definitions:

SDE3	standard deviation of elevation within a 3 km diameter circle containing the pixel at the center (m)
RE3	relative elevation (0 – 1) of a pixel within a 3 km diameter circle
S	slope, degrees
zom_flat	zom for surface in flat terrain (standard calculation), m
zom_terrain	additional roughness caused by terrain, m
zom_terrain_max	maximum terrain roughness for SDE3 >= 200 m.
aspect	aspect of slope (0 N, 180 deg. South)
aspectwind	aspect of wind (direction that wind is coming from (180 = S))

Terrain Roughness

Convective transport is increased with terrain roughness due to impacts of large scale mixing. The standard deviation of elevation (SDE) in a locality provides a good indication of the relative change in terrain elevation with distance and the associated increase in roughness and form drag.

The function derived combines, additively, roughness due to vegetation and surface features and that of larger DEM scale roughness represented by the SDE.
When not water and not agriculture, effective (adjusted) roughness is estimated as:

$$z_{om\_adj} = z_{om\_flat} + C_z \; z_{om\_terrain} \left(\frac{z_{om\_flat}}{7} + 0.3 \right)$$

where

$$z_{om\_terrain} = z_{om\_terrain\_max} \, sin\left(\frac{\pi}{2} \frac{min(SDE3, 200)}{200} \right)^3$$

with zom_terrain_max = 3 m, and with Cz = 1.0 for full effect and = 0.5 for reduced effect (used to scale impact).

The above equation for zom applies the terrain roughness increase with a baseline of 30% implementation if smooth terrain and then increasing the application according to the background (flat) roughness. The SDE is applied to a 3 km diameter circle of the 30 m DEM, with the pixel of interest at the center. The SDE3 is derived using a standard deviation tool in ERDAS. The sine function creates an “S-curve” shape for the function in terms of SDE, with maximum value for an SDE3 of 200 m and largest increase in the function at an SDE3 of 100 m.

Wind Speed increase with elevation

Wind speed is known to increase with elevated position on a slope due to convergence of flow lines and subsequent acceleration. Therefore, in sloped areas, and where SDE is significant to indicate the possibility of flow convergence, wind speed is increased as:

IF SDE3 > 30 m then

IF SDE3 < 50 m then

$$U_{200\_adj\_1} = U_{200} \, max\left(1, 1 + C_u \, RE3\left(\frac{SDE3 - 30}{50 - 30} \right) \right)$$

else

$$U_{200\_adj\_1} = U_{200} \, (1 + C_u \, RE3)$$

endif

endif

where C_u = 1.0 (coefficient). No adjustment is made when the SDE3 is less than 30 m, and is maximum when SDE3 is 50 m or more, in proportion to the relative elevation of the pixel on a slope. The relative position, RE3 is represented by the relative elevation of the point within a 3 km diameter circle. The adjustment doubles wind speed when at the highest point within a 3 km diameter when SDE3 is 50 m or greater.

Wind Speed decrease from shielding

In sloped areas, and where SDE is significant, wind speed is reduced on leeward sides of terrain due to sheltering of wind. We model this as:

IF S > 5 degrees: (i.e., if on a significant slope)

IF SDE3 > 30 m then (if in rough terrain)

IF 0.1 < RE3 < 0.95 then (if on the midslope portion of a slope)

$$U_{200\_adj\_2} = \frac{U_{200\_adj\_1}}{1 - C_s \min(0, C_a)}$$

where

$$C_a = (\sin(s))^{1.5} \, abs(\cos(aspect - aspectwind)) \cos(aspect - aspectwind)$$

else

$$C_a = 0$$

endif

else

$$C_a = 0$$

endif

else

$$C_a = 0$$

endif

where

aspect	= aspect of slope (0 N, 180 deg. South)
aspectwind	= aspect of wind (direction that wind is coming from (180 = S))
C_s	= scaling multiplier (= 4)

C_a has a range of ($-1 \le C_a \le 1$). This adjustment only occurs on leeward slopes. No adjustment occurs on windward slopes. In application, the aspect of wind direction at Agency Lake was used as a starting point for aspectwind. However, because the Agrimet weather stations are in valleys, where wind direction may be shaped somewhat by valley orientation. In addition, wind over mountains may have a regionally influenced direction that is somewhat different from that of a local weather station. We recognize that wind direction in mountains can have substantial local influence as well, according to mountain shape and orientation, up and downslope flow of air due to density differences, and valley depths and orientations. The wind aspect can, however, be used as an effective tuning parameter where the values are varied to help ET estimations on various sloped aspects to conform with expected values. This was the case for the Klamath area applications. In most cases, the apparent air flow in mountainous areas was from south to north (180 degree aspect). Values are shown in Table D-1 and D-2 for years 2004 and 2006. The impact of the reduction in wind speed can be quite strong, reducing wind speed by about 4% per 1 degree of slope on leeward faces.

Table D-1 – Values for wind aspect used to estimate areas of wind speed reduction due to shielding on leeward mountain slopes in 2004.

Image no.	**Date**	**Approximate Wind Aspect (direction) Observed at Agency Lake during the Satellite Overpass Time, deg. from North**	**Wind Aspect used in METRIC, degrees from North**

1	04/30/2004	150	150
2	06/01/2004	180	180
3	06/17/2004	shifting	180
4	07/11/2004	150	150
5	08/04/2004	150	150
6	08/20/2004	150	150
7	09/21/2004	100	180
8	10/07/2004	100	100
9	11/08/2004	100	180

Table D-2 – Values for wind aspect used to estimate areas of wind speed reduction due to shielding on leeward mountain slopes in 2006.

#	Date	Wind Aspect (0 = N), deg.
1	04/28/2006	180
2	05/06/2006	180
3	05/30/2006	180
4	06/23/2006	180
5	07/09/2006	315
6	07/25/2006	180
7	08/26/2006	180
8	09/27/2006	180
9	10/29/2006	180

Monin-Obukov boost in Aerodynamic resistance calculation on windward slopes

In sloped areas, and where SDE is significant, aerodynamic resistance, rah, is decreased on windward sides of terrain due to a boost to buoyancy-induced instability caused by the vertical component of the wind. To account for this boost:

IF S > 5 degrees then (on a slope)
IF SDE3 > 30 m then (in rough terrain):
IF stability parameter, Ψ_{z1}, Ψ_{z2} or Ψ_{200} < 0 (unstable condition) then adjust each one as

$$\Psi_{adj} = \Psi \left(+ C_{psi}\, max \left(, C_a \right) \right)$$

(increase the instability boost)
else
IF stability parameter, Ψ_{z1}, Ψ_{z2} or Ψ_{200} > 0 (stable condition) then adjust each one as

$$\Psi_{adj} = \Psi \left(- C_{psi}\, max \left(, C_a \right) \right)$$

(decrease the stability retardation)
endif
endif
endif
endif

C_{psi} is a scaling coefficient = 1.0. C_a is the same calculation as for wind sheltering (see previous section) and is a function of aspect and wind direction ($-1 \leq C_a \leq 1$).

This adjustment only occurs on windward slopes. No adjustment is made for leeward slopes. The adjustment is made for both momentum and heat transfer stability parameters and for both stable and unstable conditions.

Other adjustments

Roughness of snow

zom for snow is computed by averaging zom for pure snow and zom for the terrain. This accounts for the impact of trees, etc. protruding from the snow.

$z_{om\_snow\_cover} = (z_{om\_snow} + z_{om\_LU})/2$

ET_rF limit for snow

The METRIC energy balance uses surface temperature to estimate the near surface gradient, dT, used in the calculation of sensible heat flux, and that function implies a history of warming of the surface during early and mid-morning hours, as is characteristic of dry and evaporating surfaces. That characteristic warming is not present with snow and ice-covered surfaces, however, where surface temperature is constrained to less than or equal to 273 K. Therefore, low surface temperature of snow and ice, as opposed to nonfrozen, evaporating surfaces can cause the dT to be understated, with understatement of sensible heat flux, and therefore overstatement of ET. Therefore, in METRIC, if the estimated $ET_rF_{snow} > 0.5$, then ET_rF_{snow} is constrained to 0.5. In all likelihood, the ET is lower than this.

Appendix E. Domain of the three river basins of interest to USGS (Williamson, Wood River/Upper Klamath, and Sprague) overlaying Landsat WRS path 45/30, 44/30, and 44/31 scenes. T

he three scene areas overlapped, as shown by the colors (grey, purple and tan). Green and yellow speckles on the overlay represent agricultural and other landuses of interest. Graphic is courtesy of Daniel Snyder, USGS, Portland.